^{6}He nucleus in halo effective field theory

C. Ji, Ch. Elster, and D. R. Phillips

Phys. Rev. C **90**, 044004 — Published 31 October 2014

DOI: 10.1103/PhysRevC.90.044004

The ^{6}He Nucleus in Halo EFT

C. Ji,[1,2,*] Ch. Elster,[1,†] and D. R. Phillips[1,‡]

[1] *Institute of Nuclear and Particle Physics and Department of Physics and Astronomy, Ohio University, Athens, Ohio 45701 USA*
[2] *TRIUMF, 4004 Wesbrook Mall, Vancouver, BC V6T 2A3, Canada*[d]

(Dated: August 8, 2014)

Background: In recent years properties of light rare isotopes have been measured with high accuracy. At the same time, the theoretical description of light nuclei has made enormous progress, and properties of, e.g., the Helium isotopes can now be calculated *ab initio*. These advances make those rare isotopes an ideal testing ground for effective field theories (EFTs) built upon cluster degrees of freedom.

Purpose: Systems with widely separated intrinsic scales are well suited to an EFT treatment. The Borromean halo nucleus ^{6}He exhibits such a separation of scales. In this work an EFT in which the degrees of freedom are the valence neutrons (n) and an inert ^{4}He-core (α) is employed. The properties of ^{6}He can then be calculated using the momentum-space Faddeev equations for the αnn bound state to obtain information on ^{6}He at leading order (LO) within the EFT.

Results: The nn virtual state and the $^2\mathrm{P}_{3/2}$ resonance in ^{5}He give the two-body amplitudes which are input to our LO three-body Halo EFT calculation. We find that without a genuine three-body interaction the two-neutron separation energy S_{2n} of ^{6}He is strongly cutoff dependent. We introduce a $nn\alpha$ "three-body" operator which renormalizes the system, adjusting its coefficient to reproduce the S_{2n} of ^{6}He. The Faddeev components are then cutoff independent for cutoffs of the order of, and above, the breakdown scale of the Halo EFT.

Conclusions: As in the case of a three-body system where only resonant s-wave interactions are present, one three-body input is required for the renormalization of the EFT equations that describe ^{6}He at LO. However, in contrast to the s-wave-only case, the running of the LO $nn\alpha$ counterterm does not exhibit discrete scale invariance, due to the presence of the p-wave $n\alpha$ interaction.

PACS numbers: 21.45.-v, 21.10.Dr, 27.20.+n

[d] Permanent Address
[*] jichen@triumf.ca
[†] elster@ohio.edu
[‡] phillid1@ohio.edu

I. INTRODUCTION

The ^{6}He nucleus is a prominent example of a "halo nucleus" [1–3]. Its two-neutron separation energy, $S_{2n} = 0.975$ MeV, which is much less than the excitation energy of ^{4}He, $E^*_\alpha \approx 20$ MeV. The last two neutrons in ^{6}He thus exist in states whose probability distribution extends well beyond that of the ^{4}He core. This encourages a treatment of ^{6}He as an effective three-body problem, with ^{4}He and the two valence neutrons as degrees of freedom. In these terms ^{6}He is a Borromean system, since none of its two-body subsystems are bound, and the existence of the ^{6}He bound state is a genuine three-body phenomenon. Other neutron-rich nuclei including ^{11}Li, ^{22}C [4], and, perhaps, ^{62}Ca [5], can also be viewed as Borromean systems.

However, ^{6}He is special, since it is today accessible to *ab initio* methods which compute its structure directly from a Hamiltonian which contains state-of-the-art two-nucleon and three-nucleon interactions [6–8]. These calculations confront experimental data on S_{2n} [9] and the charge [10] and matter radii [11–13] of ^{6}He. Thus ^{6}He provides an ideal testbed to study the extent to which an effective cluster description of the halo dynamics captures essential properties of this nucleus, and when *ab initio* methods are absolutely necessary.

Descriptions of ^{6}He in a three-body ansatz have traditionally been implemented in models, with the $n\alpha$ and nn potentials determined by fitting the observed properties of the two-body subsystems. In particular, the low-energy ^{1}S$_0$ nn phase shift and the ^{2}S$_{1/2}$, ^{2}P$_{1/2}$ and ^{2}P$_{3/2}$ $n\alpha$ phase shifts were taken into consideration. In the early '70s, much work was devoted to this topic, with Ghovanlou and Lehman studying in detail which features of these phase shifts have an impact on the ^{6}He binding energy [14, 15]. They found that a model which only includes the nn resonance in the ^{1}S$_0$ channel and the "^{5}He" resonance in the ^{2}P$_{3/2}$ $n\alpha$ channel leads to overbinding of ^{6}He. The binding energy could be reduced by including other channels. Three-body cluster models of ^{6}He as a $nn\alpha$ system which included more sophisticated input for the $n\alpha$ and nn potentials were constructed in Refs. [16, 17]; two-neutron separation energies ranging from 0.68 to 0.99 MeV were found.

Cluster descriptions of halo systems are now enjoying a renaissance, thanks to the application of effective field theory (EFT) methods to these systems. EFT provides a systematic expansion in a ratio of low- to high-momentum scales. Halo nuclei enjoy a separation of these scales, since there is a low-momentum scale, M_{lo}, associated with the binding of the valence neutrons, while the high-momentum scale, M_{hi}, is set by the excitation energy of the nuclear core.

Consequently, in the case of systems where all three participating particles interact in s-waves, two-neutron halo nuclei share universal features with the three-nucleon system [18], the ^{4}He trimer [19], and cold atomic systems where three atoms interact near a Feshbach resonance. For a review of this connection see Ref. [20]. Particularly exciting is the possibility that the Efimov physics [21], having been seen experimentally in recombination rates in cold atomic gases [22–25], could also exhibit its existence in halo nuclei [26]. A variety of s-wave $2n$ halos (e.g. ^{12}Be and ^{20}C) were investigated at leading [27] and next-to-leading [28] order in the M_{lo}/M_{hi} expansion by Canham and Hammer. Recently Hagen *et al.* proposed that ^{62}Ca could also be an s-wave halo that displayed Efimovian features [5]. The existence and universal features of s-wave $2n$ halos have also been studied by Yamashita *et al.* in a renormalized zero-range model [29, 30]. Electromagnetic properties of neutron halos were analyzed in the EFT framework in Refs. [31–37].

In contrast to three-body systems including only s-wave interactions, two of the three pairwise interactions in ^{6}He are dominated by p-wave interactions. The $n\alpha$ interaction has a low-energy resonance in the ^{2}P$_{3/2}$ partial wave, as well as an enhanced phase shift in the ^{2}P$_{1/2}$ where the resonance is much broader. The first EFT treatment of $n\alpha$ scattering was carried out by Bertulani *et al.* [38], who treated both the p-wave scattering volume a_1, and the p-wave effective "range", r_1, as unnaturally enhanced—i.e. they assumed two fine tunings ($a_1 \sim 1/M_{lo}^3$, $r_1 \sim M_{lo}$). In contrast, Bedaque *et al.* [39] showed that the ^{2}P$_{3/2}$ $n\alpha$ resonance could be well described by the power counting of Ref. [40], where the resonance's width is only re-summed in its immediate vicinity. Therefore they assigned only the scaling necessary to have a low-energy resonance: $a_1 \sim 1/(M_{lo}^2 M_{hi})$, $r_1 \sim M_{hi}$, thereby requiring only one fine tuning. It is this counting we will use in our present study. We observe that the $n\alpha$ $^2P_{3/2}$ scattering parameters $a_1 = -62.951$ fm^3 and $r_1 = -0.8819$ fm^{-1} [41] are consistent with the low- and high-momentum scales $M_{lo} = \sqrt{m_N S_{2n}} \approx 30$ MeV and $M_{hi} \approx \sqrt{m_N E^*_\alpha} = 140$ MeV in ^{6}He (m_N denotes the nucleon mass).[68]

In contrast, the recent paper of Rotureau and van Kolck [43] adopted the power counting of Ref. [38], and then applied the Gamow Shell Model to solve ^{6}He as a three-body problem. In our conclusion we will compare our results with those of Ref. [43].

Another recent study of the three-body problem with resonant pairwise p-wave interactions, which employed the power counting of Ref. [38], was carried out by Braaten *et al.* [44]. These authors attempted to find a scale-free situation in the two-body problem, and examine the corresponding behavior in the three-body problem. In order to do so they took a p-wave "unitary limit" $|a_1| \to \infty$ and $r_1 \to 0$. However, as pointed out by Nishida [45] (see also Ref. [46]) this p-wave unitary limit is not physical: it yields a two-body spectrum in which one low-energy state

has negative norm. Thus the discrete scale invariance discovered by Braaten *et al.* in the corresponding three-body problem cannot be realized in nature. This provides strong motivation for us to employ the "narrow resonance" power counting $a_1 \sim 1/(M_{lo}^2 M_{hi})$, $r_1 \sim M_{hi}$ in our work.

In Sec. II, we discuss the properties of the nn and $n\alpha$ interactions employed in our work together with their low-energy expansions based on this power counting. We explain the EFT renormalization procedures which allow us to start from a two-body interaction and obtain the pertinent t-matrices. These t-matrices are then inserted into three-body Faddeev equations, for which we solve the homogeneous version in order to determine the ^{6}He ground state energy. In Sec. III we discuss the spin and angular-momentum coupling of the three particles which leads to a 0^+ state of ^{6}He. In Sec. IV we present the calculation of ^{6}He as a three-body system, building the general Faddeev equations for one spinless particle and two identical fermions, and then projecting them onto the angular-momentum channels which are relevant for the ground state of ^{6}He. We find that the ground-state energy is not determined by two-body input alone. Instead, it depends strongly on the cutoff in the three-body equations. Thus a $nn\alpha$ contact interaction is mandatory at LO in this EFT. Finally, in Sec. V, we summarize and discuss our results.

II. HALO EFT IN THE TWO-BODY SECTOR

In this section, we discuss the EFT expansion that we use for the nn and $n\alpha$ interactions,. We develop the LO two-body t-matrices, which encodes the two-body input for our three-body calculation. We discuss the regularization and renormalization procedures in both cases.

A. Halo EFT and effective-range expansions of nn and $n\alpha$ t-matrices

Here we write the Lagrangian pertaining to ^{6}He in terms of our effective $nn\alpha$ degrees of freedom. The nn part of the theory was developed as the pionless EFT in Refs. [47–49]. Successes of the pionless EFT in the nucleon-nucleon sector are summarized in the reviews [50, 51]. The $n\alpha$ part of the theory was first written down in Ref. [38] (cf. Ref. [33]). The formulation used here follows that of Ref. [37].

We write the Lagrangian $\mathscr{L}$ as a sum of one-body, two-body, and three-body terms.

$$\mathscr{L} = \mathscr{L}_1 + \mathscr{L}_2 + \mathscr{L}_3 \ . \tag{1}$$

The one-body Lagrangian $\mathscr{L}_1$ is

$$\mathscr{L}_1 = n^\dagger \left(i\partial_0 + \frac{\nabla^2}{2m_n} \right) n + \alpha^\dagger \left(i\partial_0 + \frac{\nabla^2}{2m_\alpha} \right) \alpha \ , \tag{2}$$

where α is the spinless field of ^{4}He with mass m_α, and $n^\dagger$ is the two-component spinor field of the valence neutron $n^\dagger = \binom{n_\uparrow}{n_\downarrow}$ with mass m_n. The two-body Lagrangian $\mathscr{L}_2$ include the nn s-wave and $n\alpha$ p-wave interactions:

$$\begin{aligned} \mathscr{L}_2 =& \eta_0 \, s^\dagger \left(i\partial_0 + \frac{\nabla^2}{4m_n} - \Delta_0 \right) s + \eta_1 \, \pi^\dagger \left(i\partial_0 + \frac{\nabla^2}{2(m_n + m_\alpha)} - \Delta_1 \right) \pi \\ &+ g_0 \left[s^\dagger T_0^{\sigma\delta} n_\sigma n_\delta + \text{h.c.} \right] + g_1 \left[\pi^{\dagger a} T_a^{\sigma i} \left(n_\sigma \overleftrightarrow{\partial}_i \alpha \right) + \text{h.c.} \right], \end{aligned} \tag{3}$$

where $\eta_0 = \eta_1 = \pm 1$, with the sign determined respectively by the s- and p-wave effective ranges. s is the spin-singlet auxiliary field of the nn pair, π_a is the four-component field for the $^2P_{3/2}$ resonance in the $n\alpha$ system. $\overleftrightarrow{\partial}_i \equiv [(\overleftarrow{m}\overleftarrow{\nabla} - \overleftarrow{m}\overrightarrow{\nabla})/(\overleftarrow{m} + \overrightarrow{m})]_i$ indicates the Galilean invariant derivative, where $\overleftarrow{m}$ (or $\overrightarrow{m}$) is the mass of the field operated by $\overleftarrow{\nabla}$ (or $\overrightarrow{\nabla}$). Following the convention of Ref. [37], we define the spin projections of the fields and operators by their indices with $\sigma, \delta, .. = \pm 1/2$, $a, b, .. = \pm 1/2, \pm 3/2$, and $i, j, .. = 0, \pm 1$. $T_{...}^{...}$ is the shorthand notation for the Clebsch-Gordan coefficient, e.g., $T_a^{\sigma i} = T_{\sigma i}^a \equiv C(1/2, 1, 3/2 \,|\, \sigma \, i \, a)$.

The three-body Lagrangian $\mathscr{L}_3$ describes the $nn\alpha$ contact interaction, whose existence and specific form are derived as a consequence of three-body renormalization (see Sec. IV).

$$\mathscr{L}_3 = -h \left(T_0^{ab} T_a^{i\sigma} \pi_b \overleftrightarrow{\partial}_i n_\sigma \right)^\dagger \left(T_0^{cd} T_c^{j\delta} \pi_d \overleftrightarrow{\partial}_j n_\delta \right) \tag{4}$$

The nn interaction is dominated by an s-wave virtual state, where the scattering length, $a_0 = -18.7$ fm [52], is approximately one order of magnitude larger than the corresponding effective range, $r_0 = 2.75$ fm [53]. According to

the effective-range expansion at low energies, the nn t-matrix for elastic scattering can be written up to second order in the expansion in powers of M_{lo}/M_{hi} as

$$\langle \boldsymbol{k}|t_{nn}|\boldsymbol{k'}\rangle = -\frac{1}{4\pi^2\mu_{nn}}\,\frac{1}{k\cot\delta_0 - ik} = \frac{1}{4\pi^2\mu_{nn}}\,\frac{1}{1/a_0 - r_0k^2/2 + ik}\ , \tag{5}$$

where μ_{nn} is the reduced mass in the nn center-of-mass (c.m.) frame, $k \equiv |\boldsymbol{k}| = |\boldsymbol{k'}| = \sqrt{2\mu_{nn}E}$ indicates the on-shell relative momentum in the nn subsystem, and E is the two-body energy. Terms with higher powers of k, such as shape-dependent terms in the effective-range expansion, are suppressed at low momentum. The free state $|\boldsymbol{p}\rangle$ is normalized as

$$\langle \boldsymbol{p}|\boldsymbol{p'}\rangle = \delta^{(3)}(\boldsymbol{p}-\boldsymbol{p'})\ . \tag{6}$$

The result (5) is an exact result for the nn t-matrix, given the Lagrangians (2) and (3). For the relationship between the Lagrangian parameters and the effective-range parameters, see, e.g. Ref. [37].

Similarly to the power counting employed in short-range EFT (SREFT) for boson-boson s-wave scattering, a_0, is associated with the low-momentum scale, $a_0 \sim 1/M_{lo}$, while r_0 is related to the high-momentum scale of short-distance physics, $r_0 \sim 1/M_{hi}$. At leading order (LO) in an expansion in powers of M_{lo}/M_{hi}, the position of the nn s-wave virtual state (since $a_0 < 0$) is given by $\gamma_0 = 1/a_0$. Hereafter the LO t-matrix for nn scattering is written as

$$\langle \boldsymbol{k}|t_{nn}|\boldsymbol{k'}\rangle = \frac{1}{4\pi^2\mu_{nn}(\gamma_0 + ik)}\ , \tag{7}$$

where the r_0 dependent term in Eq. (5) is dropped at LO.

The $n\alpha$ interaction is dominated by a p-wave resonance. Based on the p-wave effective-range expansion at low energies, the dominant part of the $n\alpha$ t-matrix can be expressed as

$$\langle \boldsymbol{k}|t_{n\alpha}|\boldsymbol{k'}\rangle = -\frac{3}{4\pi^2\mu_{n\alpha}}\,\frac{\boldsymbol{k}\cdot\boldsymbol{k'}}{k^3\cot\delta_0 - ik^3} = \frac{3}{4\pi^2\mu_{n\alpha}}\,\frac{\boldsymbol{k}\cdot\boldsymbol{k'}}{1/a_1 - r_1k^2/2 + ik^3}, \tag{8}$$

where $k = \sqrt{2\mu_{n\alpha}E}$, and $\mu_{n\alpha}$ is the reduced mass in the $n\alpha$ c.m. frame. Eq. (8) is the full result for the $n\alpha$ t-matrix, given the Lagrangians (2) and (3). The relationship between p-wave effective-range and Lagrangian parameters can be deduced from the results of Ref. [33].

Here we adopt the power-counting of Bedaque *et al.* [39], who assumed $1/a_1 \sim M_{lo}^2 M_{hi}$ and $r_1 \sim M_{hi}$. Based on this power counting, the $n\alpha$ interaction has a narrow resonance at a low energy of order M_{lo}, with the co-existence of a deep bound state $\sim M_{hi}$. We see this by decomposing the denominator of Eq. (8) based on its pole expansion:

$$\frac{1}{a_1} - \frac{1}{2}r_1k^2 + ik^3 = (\gamma_1 + ik)\left(k^2 + i\frac{k_R^2}{\gamma_1}k - k_R^2\right) = 0\ , \tag{9}$$

where γ_1 indicates the position of the bound-state pole, and k_R is the resonant momentum. The position of the resonance, together with its width, is determined from Eq. (9) as

$$k_\pm = \pm k_R\sqrt{1 - \frac{k_R^2}{4\gamma_1^2}} - i\frac{k_R^2}{2\gamma_1}\ . \tag{10}$$

From Eq. (9), we can relate γ_1 and k_R to a_1 and r_1 by

$$\frac{1}{a_1} = -\gamma_1 k_R^2 \tag{11a}$$

$$\frac{r_1}{2} = \frac{k_R^2}{\gamma_1} - \gamma_1\ . \tag{11b}$$

Based on the power-counting introduced above, we obtain that $\gamma_1 \sim M_{hi}$ and $k_R \sim M_{lo}$.

The deep bound state $\gamma \sim M_{hi}$ does not affect low-energy physics. Meanwhile, the resonance poles can be rewritten in the M_{lo}/M_{hi} expansion as

$$k_\pm = \pm k_R - ik_R^2/(2\gamma_1) + \mathcal{O}(M_{lo}^3/M_{hi}^2). \tag{12}$$

The resonance width (imaginary part) is thus one order higher than the resonance position (real part).

Unless we happen to be in the vicinity of the resonance, we then obtain, at LO:

$$\gamma_1 = -\frac{r_1}{2} \tag{13}$$

$$k_R = \sqrt{\frac{2}{a_1 r_1}} \ . \tag{14}$$

Therefore, the LO part of the $n\alpha$ scattering t-matrix is expressed as

$$\langle \boldsymbol{k}|t_{n\alpha}|\boldsymbol{k'}\rangle = \frac{3\boldsymbol{k}\cdot\boldsymbol{k'}}{4\pi^2\mu_{n\alpha}\gamma_1(k^2-k_R^2)} \ , \tag{15}$$

where the unitary term ik^3 in Eq. (8) is treated as a perturbation and is dropped at LO. Note that the deep bound state does not appear in this LO amplitude: this t-matrix only has two poles, at $k = \pm k_R$ on the real k-axis, which correspond to the resonance. Since here we are only interested in the bound-state ^{6}He, the energy of the $n\alpha$ subsystem must be negative ($k^2 < 0$). Therefore the singularity in Eq. (15) does not cause any numerical issues in our calculations.

B. Partial-wave decomposition of the two-body t-matrix

In this subsection we explicitly give the partial wave decomposition of the two-body t-matrix in order to establish our conventions. The momentum space Lippmann-Schwinger equation is given by

$$\langle \boldsymbol{p}|t(E)|\boldsymbol{p'}\rangle = \langle \boldsymbol{p}|V|\boldsymbol{p'}\rangle + \int d^3q\, \langle \boldsymbol{p}|V|\boldsymbol{q}\rangle G_0(q;E)\langle \boldsymbol{q}|t(E)|\boldsymbol{p'}\rangle \ , \tag{16}$$

where $\boldsymbol{p}$ and $\boldsymbol{p'}$ denote the two-body relative momenta, G_0 is the free Green's function in the two-body system. Defining partial-wave components of the potential, $v_l(p,p')$, via

$$v_l(p,p') \equiv \frac{1}{2}\int_{-1}^{1} \langle \boldsymbol{p}|V|\boldsymbol{p'}\rangle \, \mathrm{P}_l(\hat{\boldsymbol{p}}\cdot\hat{\boldsymbol{p}}')\, d(\hat{\boldsymbol{p}}\cdot\hat{\boldsymbol{p}}') \ , \tag{17}$$

where P_l is the lth Legendre polynomial, and analogously for $t_l(p,p';E)$, we obtain

$$t_l(p,p';E) = v_l(p,p') + 4\pi\int_0^\infty dq\, q^2 v_l(p,q)\, G_0(q;E)\, t_l(q,p';E) \ . \tag{18}$$

In our case all two-body interactions have a resonance in one particular partial wave, which dominates the behavior of the t-matrix. Considering only the dominant part, we have

$$\langle \boldsymbol{p}|t(E)|\boldsymbol{p'}\rangle = (2l+1)\, t_l(p,p';E)\, \mathrm{P}_l(\hat{\boldsymbol{p}}\cdot\hat{\boldsymbol{p}}') \ , \tag{19}$$

with $l = 0$ and 1 indicating the s- and p-wave two-body interactions. To simplify the calculation, we will study $t_l(p,p';E)$ using the formalism of separable potentials. Here we define the lth partial wave of the Hermitian two-body potential in a separable form as

$$v_l(p,p') = \lambda_l\, g_l(p)\, g_l(p') \ , \tag{20}$$

where $g_l(q)$ is the form factor, which only depends on the magnitude of $\boldsymbol{q}$. By substituting Eq. (20) into Eq. (19), $t_l(p,p';E)$ is then also separable,

$$t_l(p,p';E) = g_l(p)\, \tau_l(E)\, g_l(p') \ , \tag{21}$$

where the function τ_l is given as

$$\tau_l^{-1}(E) = \frac{1}{\lambda_l} - 4\pi\int_0^\infty dq\, \frac{q^2}{E - q^2/(2\mu) + i\epsilon} g_l^2(q) \ , \tag{22}$$

and only depends on the energy E of the two-body system.

To reproduce the physical two-body scattering amplitude, the integral in Eq. (22) needs to be regularized and renormalized. For a particular partial wave, the low-energy behavior of the two-body t-matrix is determined by the effective-range expansion. By choosing a particular form factor g_l we can regulate the integral in Eq. (22) and then tune the two-body coupling constant λ_l to absorb the resulting regularized divergence, thereby reproducing the parameters in the effective-range expansion. By doing so, the t-matrix is renormalized, and the dependence of the low-energy physics on the choice of $g_l(q)$ disappears.

C. Two-body renormalization with a separable potential

One regularization method is to introduce Yamaguchi form factor to describe the two-body interaction, i.e. writing the form factor as

$$g_l(q) = \frac{\beta_l^{2(l+1)}}{(q^2+\beta_l^2)^{l+1}}\, q^l \ . \tag{23}$$

Here β_l indicates the high-momentum scale that regularizes the integrals in Eq. (22). The renormalization of the two-body t-matrix using such a potential is discussed in Appendix A. Already forty years ago, Ghovanlou and Lehman in [14] used these form factors to represent the two-body short-distance physics, hoping to determine three-body observables in ^{6}He without the input of three-body parameters. However, their value of the ^{6}He ground-state binding energy underpredicts the experimental value. The introduction of a three-body force may be a more effective way to obtain an accurate description of the ^{6}He nucleus using simple two-body potentials. After all, low-energy three-body physics is insensitive to short-distance details of the input two- and three-body interactions.

In this section we introduce a hard cutoff, Λ, to regularize the ultraviolet divergence in Eq. (22),

$$g_l(p) = p^l \theta(\Lambda - p) \ , \tag{24}$$

where $\theta(x)$ denotes the Heaviside step function: $\theta(x) = 0$ for $x < 0$, and 1 for $x > 0$.

For the s-wave nn interaction ($l = 0$) we obtain

$$\begin{aligned}\langle \boldsymbol{k}|t_{nn}|\boldsymbol{k}'\rangle =& \tau_{nn}(E) \\ =& \left[\frac{1}{\lambda_0} + 8\pi\mu_{nn}\int_0^\Lambda dq\, \frac{q^2}{(q^2-k^2-i\epsilon)}\right]^{-1} \\ =& \frac{1}{4\pi^2\mu_{nn}}\left[\frac{1}{4\pi^2\mu_{nn}\lambda_0} + \frac{2\Lambda}{\pi} - \frac{2}{\pi\Lambda}k^2 + ik + \mathcal{O}\left(\frac{k^3}{\Lambda^2}\right)\right]^{-1} \ .\end{aligned} \tag{25}$$

We can relate a_0 and r_0 to λ_0 and Λ by

$$\frac{1}{a_0} = \frac{1}{4\pi^2\mu_{nn}\lambda_0} + \frac{2\Lambda}{\pi} \ , \tag{26a}$$

$$\frac{r_0}{2} = \frac{2}{\pi\Lambda} \ . \tag{26b}$$

By tuning λ_0 in Eq. (26a) to cancel the divergent piece $\sim \Lambda$, we can obtain a_0 of order $1/M_{lo}$. Eq. (26b) shows that the condition $r_0 \sim 1/M_{hi}$ is naturally maintained if we keep $\Lambda \sim M_{hi}$. But physics is independent of Λ if additional higher-order terms are included in $\mathscr{L}$. Therefore, we obtain the renormalized τ_{nn} in the limit $\Lambda \to \infty$ as

$$\tau_{nn}(E) = \frac{1}{4\pi^2\mu_{nn}(\gamma_0 + ik)} \ , \tag{27}$$

where $k = \sqrt{2\mu E}$. This corresponds to the leading-order t-matrix of Eq. (7).

In the case of p-wave ($l = 1$) $n\alpha$ scattering Eq. (24) leads to a regularized t-matrix for $n\alpha$ scattering,

$$\begin{aligned}\langle \boldsymbol{k}|t_{n\alpha}|\boldsymbol{k}'\rangle =& 3\boldsymbol{k}\cdot\boldsymbol{k}'\,\tau_{n\alpha}(E) \\ =& \frac{3\boldsymbol{k}\cdot\boldsymbol{k}'}{4\pi^2\mu_{n\alpha}}\left(\frac{1}{4\pi^2\mu_{n\alpha}\lambda_1} + \frac{2\Lambda^3}{3\pi} + \frac{2\Lambda}{\pi}k^2 + ik^3 + \cdots\right)^{-1} \ .\end{aligned} \tag{28}$$

In order to renormalize $t_{n\alpha}$ with one fine-tuning, a_1 and r_1 must satisfy

$$\frac{1}{a_1} = \frac{1}{4\pi^2\mu_{n\alpha}\lambda_1} + \frac{2\Lambda^3}{3\pi} \ , \tag{29a}$$

$$\frac{r_1}{2} = -\frac{2\Lambda}{\pi} \ . \tag{29b}$$

Eq. (29b) indicates that $r_1 \sim M_{hi}$, which agrees with the power-counting analysis in Ref. [39]. After tuning λ_1 to cancel the $\sim \Lambda^3$ divergence, we reproduce a_1 to its physical value. Since $a_1 \sim 1/(M_{lo}^2 M_{hi})$, it has the same order as

TABLE I. Spin and orbital-angular-momentum coupling in ^{6}He to obtain its ground state $J = 0^+$.

(spectator,pair)	pair	spectator	total L, S	total J^P
(α,nn)	$\ell_\alpha = 0$, $s_\alpha = 0$	$\lambda_\alpha = 0$, $\sigma_\alpha = 0$	$L_\alpha = 0$, $S_\alpha = 0$	$J = 0^+$
(n,$n\alpha$)	$\ell_n = 1$, $s_n = \frac{1}{2}$	$\lambda_n = 1$, $\sigma_n = \frac{1}{2}$	$L_n = 0$, $S_n = 0$	
			$L_n = 1$, $S_n = 1$	

the $r_1 k^2/2$ term in the effective-range expansion. Therefore, the p-wave effective-range parameter r_1 must be included at leading order, which agrees with our previous analysis in Subsection II A.

Thus, after renormalization, we find for $\tau_{n\alpha}$

$$\tau_{n\alpha} = \frac{1}{4\pi^2 \mu_{n\alpha} \gamma_1 (k^2 - k_R^2)} \ . \tag{30}$$

In contradistinction, the power counting of Ref. [38] with $a_1 \sim M_{lo}^{-3}$ and $r_1 \sim M_{lo}$ requires two fine tunings in Eq. (28) to renormalize $t_{n\alpha}$, and yields a different LO expression for $\tau_{n\alpha}$.

III. SPIN AND ANGULAR MOMENTA IN THE ^{6}HE GROUND STATE

The ground-state of ^{6}He has total angular momentum and parity $J = 0^+$. Its two-neutron separation energy is 0.975 MeV. In this paper we will use Jacobi-momenta $\boldsymbol{K}$, $\boldsymbol{q}_i$, and $\boldsymbol{p}_i$ to represent the internal kinematics of the three-body system. Here $\boldsymbol{K}$ is the total momentum, which is zero in the c.m. frame, and $\boldsymbol{q}_i$ and $\boldsymbol{p}_i$ are the relative momenta. The index i on the relative momenta indicates that they are defined in the two-body fragmentation channel (i, jk), in which particle i is the spectator and (jk) the interacting pair. Based on this definition, $\boldsymbol{p}_i$ indicates the relative momentum in the (jk) pair, while $\boldsymbol{q}_i$ denotes the relative momentum between the spectator i and the (jk) pair. Plane-wave states are normalized according to:

$$\int d\boldsymbol{p}_i d\boldsymbol{q}_i d\boldsymbol{K} |\boldsymbol{p}_i \boldsymbol{q}_i \boldsymbol{K}\rangle\langle \boldsymbol{p}_i \boldsymbol{q}_i \boldsymbol{K}| = \mathbb{1}. \tag{31}$$

We define the relative orbital angular momentum and the spin in the pair (jk) as l_i and s_i, and the relative total angular momentum for this pair in spin–and–orbital-angular-momentum coupling as j_i. In this representation, we also define the relative orbital angular momentum and spin between the spectator i and the pair (jk) as λ_i and σ_i, and the corresponding total angular momentum as I_i. Furthermore, the overall orbital angular momentum, spin and total angular momentum of the three-body system are defined as L_i, S_i and J. Due to spin and angular-momentum conservation, these quantum numbers must obey

$$\boldsymbol{L}_i = \boldsymbol{l}_i + \boldsymbol{\lambda}_i \ , \tag{32a}$$

$$\boldsymbol{S}_i = \boldsymbol{s}_i + \boldsymbol{\sigma}_i \ , \tag{32b}$$

$$\boldsymbol{J} = \boldsymbol{L}_i + \boldsymbol{S}_i = \boldsymbol{j}_i + \boldsymbol{I}_i \ . \tag{32c}$$

With the α-core as the spectator, we obtain $l_\alpha = s_\alpha = j_\alpha = 0$, since the nn interaction is dominated by the ^{1}S$_0$ virtual state. Furthermore, at LO $\lambda_\alpha = \sigma_\alpha = I_\alpha = 0$ and it is then straightforward to determine that $S_\alpha = L_\alpha = 0$ in the (α, nn) partition. Alternatively, if we choose a neutron as the spectator, the $n\alpha$ interaction is dominated by the ^{2}P$_{3/2}$ resonance, which means $l_n = 1$, $s_n = 1/2$ and $j_n = 3/2$. Therefore, in ^{6}He ground state, the spectator neutron must also interact with the $n\alpha$ pair in a p-wave, because of the positive parity of the ^{6}He ground state. This results in $\lambda_n = 1$, $\sigma_n = 1/2$. Since $\boldsymbol{j}_n + \boldsymbol{I}_n = \boldsymbol{J} = 0$, we must have $I_n = 3/2$. In the $(n, n\alpha)$ partition, the spin-spin and orbit-orbit couplings have two possibilities: the overall orbital angular momentum and overall spin can either be both zero ($L_n = S_n = 0$) or both one ($L_n = S_n = 1$). These two cases can contribute to the ^{6}He $J = 0^+$ state. We summarize the possible spin and orbital-angular-momentum properties of the ^{6}He ground state in Table III with respect to different spectator partitions.

Knowing the spin and orbital-angular-momentum quantum numbers, we can construct an eigenstate of ^{6}He with respect to the spin and orbital-angular-momentum operators. Considering all conserved quantities in the three-body

system, we decompose the Jacobi momenta with respect to these spin and orbital- and total-angular-momentum quantum numbers by

$$|p,q;\Omega_i\rangle_i = \sum_{L_i S_i} \sqrt{\widehat{j}_i \widehat{I}_i \widehat{L}_i \widehat{S}_i} \begin{Bmatrix} l_i & s_i & j_i \\ \lambda_i & \sigma_i & I_i \\ L_i & S_i & J \end{Bmatrix} |p,q;(l_i,\lambda_i)L_i\,;[(\nu_j\nu_k)s_i,\sigma_i]\,S_i\,;J=M_J=0\rangle_i \ , \tag{33}$$

where $\widehat{j}_i$ denotes $2j_i+1$ (the same holds for $\widehat{I}_i$, $\widehat{L}_i$ and $\widehat{S}_i$), $p \equiv |\boldsymbol{p}|$, and $q \equiv |\boldsymbol{q}|$. Meanwhile Ω_i represents all conserved spin, orbital- and total-angular-momentum quantum numbers in the partition (i,jk). Those quantum numbers are included in the Wigner 9j symbol in Eq. (33). In addition, the labels ν_j and ν_k in the bracket denote the individual spins of particle j and k. They are coupled to produce the spin s_i of the pair (jk).

Applying Eq. (33) in the partition (α,nn) the eigenstate of the ^{6}He ground state can be written as

$$|p,q;\Omega_\alpha\rangle_\alpha = \left| p,q;\,(0,0)L_\alpha=0;\,\left[\left(\frac{1}{2}\frac{1}{2}\right)0,0\right]S_\alpha=0;\,J=M_J=0\right\rangle_\alpha \ . \tag{34}$$

Similarly, in the partition $(n,n\alpha)$, the ^{6}He ground-state eigenstate can be expressed as

$$|p,q;\Omega_n\rangle_n = \sum_{L_n=0}^{1} \sqrt{\frac{2}{3}}\left(\frac{-1}{\sqrt{2}}\right)^{L_n} \left| p,q;\,(1,1)L_n;\,\left[\left(\frac{1}{2}0\right)\frac{1}{2},\frac{1}{2}\right]S_n=L_n;\,J=M_J=0\right\rangle_n \ . \tag{35}$$

We can further decouple the orbital angular momentum and the spin by using the Clebsch-Gordan coefficient $C(LSJ|M_L M_S M_J)$. In the (α,nn) basis we obtain

$$|p,q;\Omega_\alpha\rangle_\alpha = |p,q;\,0,0;L_\alpha=0,M_{L\alpha}=0\rangle_\alpha \left|\left(\frac{1}{2}\,\frac{1}{2}\right)\,0,0;S_\alpha=0,M_{S\alpha}=0\right\rangle_\alpha \ , \tag{36}$$

while in the $(n,n\alpha)$ basis, we find

$$|p,q;\Omega_n\rangle_n = \sum_{L_n=0}^{1}\sum_{M_{Ln}=-L_n}^{L_n} (-1)^{M_{Ln}}\sqrt{\frac{2^{1-L_n}}{6L+3}}\,|p,q;\,1,1;\,L_n,M_{Ln}\rangle_n \left|\left(\frac{1}{2}0\right)\frac{1}{2},\frac{1}{2};\,S_n=L_n,M_{Sn}=-M_{Ln}\right\rangle_n \ . \tag{37}$$

IV. HALO EFT IN THE THREE-BODY SECTOR

In this section, we study the behavior of ^{6}He as a three-body problem in halo EFT. We focus on the three-body bound-state problem, and set up the Faddeev equations, based on Refs. [54, 55], for solving for the three-body binding energy of ^{6}He. We then employ the formalism to investigate the ground state of ^{6}He projected on to the particular partial waves discussed in Sec. III. Without a $nn\alpha$ three-body counterterm, the results will be cutoff dependent. Therefore, we need to discuss the regularization and renormalization procedures in our analysis. By adding a $nn\alpha$ counterterm, we reproduce the experimental value of the ^{6}He two-neutron separation energy, $S_{2n} = 0.975$ MeV, and predict the Faddeev components.

A. Faddeev decomposition of the three-body wave function

Considering only two-body potentials, the general Schrödinger equation in a system with three distinguishable particles reads

$$\left(H_0 + \sum_{i=1}^{3} V_i\right)|\Psi\rangle = E\,|\Psi\rangle \ , \tag{38}$$

where V_i indicates the potential between particles j and k, that in the partition (i,jk). Following Faddeev [56], the wave function is decomposed into three components, one with respect to each of the three different spectators,

$$|\Psi\rangle = \sum_{i=1}^{3} |\psi_i\rangle \ , \tag{39}$$

with $|\psi_i\rangle$ being the Faddeev component in the (i, jk) partition. Inserting Eq. (39) into Eq. (38) and employing the Lippmann-Schwinger equation we obtain [54]

$$|\psi_i\rangle = G_0 t_i \sum_{j\neq i} |\psi_j\rangle \ . \tag{40}$$

Here t_i represents the two-body t-matrix for the pair (jk), $t_i \equiv t_{jk}$. All components are obtained by a cyclic permutation of (i, jk). Note that Eq. (40) is a homogeneous integral equation, since only the bound state is considered.

To simplify our future calculations, we define new components $|F_i\rangle$, which are related to $|\psi_i\rangle$ by

$$|\psi_i\rangle = G_0 t_i |F_i\rangle \ . \tag{41}$$

By substituting Eq. (41) into Eq. (40), we obtain the Faddeev equation for $|F_i\rangle$:

$$|F_i\rangle = \sum_{j\neq i} G_0 t_j |F_j\rangle \ . \tag{42}$$

If the two-body t-matrix, t_i, is separable, then its matrix presentation in the basis of eigenstates $\{\, |p, q, ; \Omega_i\rangle_i\}$ leads to a relatively simple expression in which the momenta p, p', and q are decoupled,

$${}_i\langle p, q; \Omega_i | t_i | p', q'; \Omega_i'\rangle_i = 4\pi \, g_{l_i}(p) \, \tau_i(q; E) \, g_{l_i}(p') \, \delta_{\Omega_i \Omega_i'} \, \frac{1}{q^2} \delta(q - q') \ , \tag{43}$$

provided that the two-body t-matrix is diagonal in the quantum numbers Ω_i. In our case t_i operates only in a specific partial wave: ${}^1\mathrm{S}_0$ for nn and ${}^2\mathrm{P}_{3/2}$ for $n\alpha$. Eq. (43) only gives the two-body t-matrix's matrix elements in three-body Hilbert space when Ω_i corresponds to those particular two-body channels. The matrix elements in all other channels are zero in our LO calculation. The quantity τ_i in Eq. (43) is related to τ_{jk} of Eqs. (27) and (30) by

$$\tau_i(q; E) \equiv \tau_{jk}\left(E - \frac{q^2}{2\mu_{i(jk)}}\right) \ . \tag{44}$$

Here E denotes the total energy of the three-body system relative to the αnn threshold, and $\mu_{i(jk)}$ is the reduced mass with respect to the spectator i and the pair (jk). We are interested in $E = -B_3$, with $B_3 > 0$ the binding energy of the three-body system, which, for two-neutron halos, is the two-neutron separation energy of the nucleus, i.e., $B_3 = S_{2n}$.

Projecting Eq. (42) on to the state $|p, q; \Omega_i\rangle_i$ leads to

$$\begin{aligned} {}_i\langle p, q; \Omega_i | F_i\rangle =& 4\pi \sum_{j\neq i} \iint p'^2 dp' \, q'^2 dq' \, G_0^{(i)}(p, q; E) \ {}_i\langle p, q; \Omega_i | p', q'; \Omega_j\rangle_j g_{l_j}(p') \, \tau_j(q'; E) \\ & \times \int p''^2 dp'' \, g_{l_j}(p'') \, {}_j\langle p'', q'; \Omega_j | F_j\rangle \ , \end{aligned} \tag{45}$$

where $G_0^{(i)}$ is the momentum representation of the three-body Green's function with respect to the spectator i:

$$G_0^{(i)}(p, q; E) = \left(E - \frac{p^2}{2\mu_{jk}} - \frac{q^2}{2\mu_{i\,(jk)}}\right)^{-1} \ . \tag{46}$$

Absorbing the dependence on the inter-pair momentum, p, in the Faddeev equation (45), we can construct a simplified integral equation in which quantities depend only on the relative momentum between the spectator and the pair, q. To achieve this, we define a new function $F_i(q)$,

$$F_i(q) = \int p^2 dp \, g_{l_i}(p) \ {}_i\langle p, q; \Omega_i | F_i\rangle \ . \tag{47}$$

By substituting Eq. (47) into Eq. (45), we find that

$$F_i(q) = \sum_{j\neq i} 4\pi \int q'^2 dq' \, X_{ij}(q, q'; E) \, \tau_j(q'; E) \, F_j(q') \ . \tag{48}$$

The kernel function X_{ij} is defined by

$$X_{ij}(q,q';E) = \iint p^2 dp\, p'^2 dp'\, g_{l_i}(p) G_0^{(i)}(p,q;E)\, g_{l_j}(p')\ {}_i\langle p,q;\Omega_i|p',q';\Omega_j\rangle_j\ , \tag{49}$$

which includes the three-body Green's function $G_0^{(i)}$ and the two-body form factors g_{l_i} and g_{l_j}. The factor ${}_i\langle p,q;\Omega_i|p',q';\Omega_j\rangle_j$ is the projection of the eigenstate of the free Hamiltonian in the partition of spectator i onto the free eigenstate in the partition of spectator j [54].

To solve this integral equation (48), we look for an energy $E = -B_3$ where the eigenvalue of the kernel is one.

B. Faddeev equations for the ^{6}He system

Here we apply the Faddeev formalism established in the previous subsection to the ^{6}He ground state. For this purpose Eq. (39) can be re-expressed as

$$|\Psi\rangle = |\psi_\alpha\rangle + |\psi_n\rangle + |\psi_{n'}\rangle = |\psi_\alpha\rangle + (1-\mathcal{P}_{nn})|\psi_n\rangle\ , \tag{50}$$

where the three terms are the Faddeev components for (α, nn), and the two $(n, n\alpha)$ partitions, with those last two related by fermionic symmetry. Because the two neutrons are fermions the ^{6}He wave function must be anti-symmetric under their permutation $\mathcal{P}_{nn}$, and Eq. (50) indeed fulfils

$$\mathcal{P}_{nn}|\Psi\rangle = -|\Psi\rangle, \tag{51}$$

since

$$\mathcal{P}_{nn}|\psi_\alpha\rangle = -\,|\psi_\alpha\rangle. \tag{52}$$

The Green's function, G_0, and the two-body t-matrices t_α and t_n are unchanged under the action of $\mathcal{P}_{nn}$, because they were defined above as projections of only the neutron-spin-independent part of the eigenstate.

By projecting the Faddeev components $|F_\alpha\rangle$ and $|F_n\rangle$ onto the partial-wave-decomposed states in respective partitions we obtain two coupled-channel integral equations for the ^{6}He ground state,

$$F_\alpha(q) = 8\pi \int_0^\Lambda q'^2 dq'\, X_{\alpha n}(q,q';-B_3)\, \tau_n(q';-B_3)\, F_n(q')\ ; \tag{53a}$$

$$F_n(q) = 4\pi \int_0^\Lambda q'^2 dq'\, X_{n\alpha}(q,q';-B_3)\, \tau_\alpha(q';-B_3)\, F_\alpha(q') + 4\pi \int_0^\Lambda q'^2 dq'\, X_{nn}(q,q'-B_3)\, \tau_n(q';-B_3)\, F_n(q')\ , \tag{53b}$$

where the ultraviolet cutoff, Λ, is introduced for regularization. The Faddeev equations (53a, 53b) are diagrammatically expressed in Fig. 1. Similar coupled-channel integral equations for two-neutron s-wave halo nuclei were derived by Canham and Hammer in Ref. [27], where the two sets of equations differ only in their expressions for the kernel functions X_{ij}.

The quantities τ_α and τ_n appearing in Eqs. (53a) and (53b) are functions of the ^{6}He two-neutron separation energy B_3 and the Jacobi momentum q:

$$\tau_\alpha(q;-B_3) = \frac{1}{2\pi^2 m_n} \frac{1}{\gamma_0 - \mathcal{K}_\alpha(q;-B_3)}\ , \tag{54}$$

where the two-body binding momentum $\mathcal{K}_\alpha$ is related to q and B_3 by

$$\mathcal{K}_\alpha(q;-B_3) = \sqrt{m_n B_3 + \frac{A+2}{4A} q^2}\ . \tag{55}$$

Here A indicates the mass ratio between the α-core and a neutron $A = m_\alpha/m_n$.

Similarly, we can write τ_n as a function of B_3 and the Jacobi momentum q:

$$\tau_n(q;-B_3) = -\frac{1}{4\pi^2 m_n \gamma_1} \left(\frac{A+1}{A}\right) \frac{1}{\mathcal{K}_n^2(q;-B_3) + k_R^2}\ , \tag{56}$$

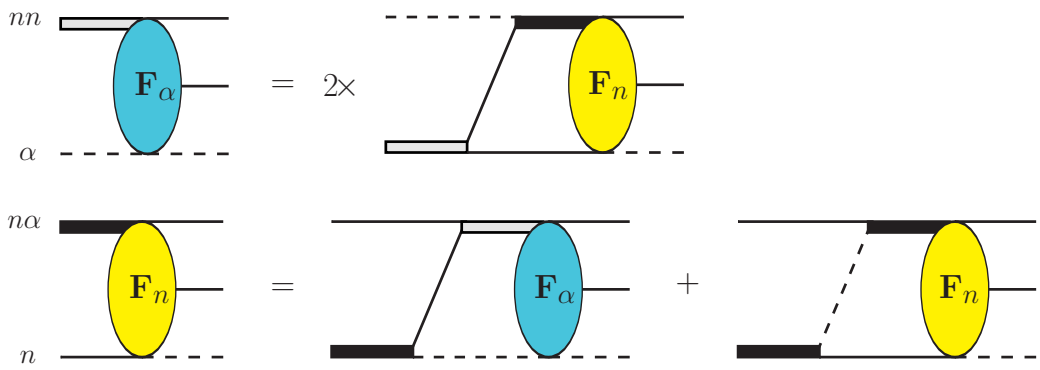

FIG. 1. (Color online) The Faddeev equations for the ^{6}He bound-state problem: The single dashed (or solid) line denotes the α (or n) one-body propagator. The thick black and shaded lines represents the $n\alpha$ and nn two-body propagators. The ellipses labeled "F_α" and "F_n" are the corresponding Faddeev components.

where $\mathcal{K}_n$ is given as

$$\mathcal{K}_n(q;-B_3) = \sqrt{\frac{2A}{A+1}\left(m_n B_3 + \frac{A+2}{2(A+1)}q^2\right)} \,. \tag{57}$$

Meanwhile the kernel functions $X_{n\alpha}$, $X_{\alpha n}$ and X_{nn} are calculated according to Eq. (49), where the subscripts indicate the two spectator partitions involved in the transition. The details of these calculations are presented in Appendix B, and result in the final expressions:

$$X_{n\alpha}(q,q';-B_3) = -\sqrt{2}\, m_n \left[\frac{A}{A+1}\frac{1}{q'}\,\mathrm{Q}_0(z_{n\alpha}) + \frac{1}{q}\,\mathrm{Q}_1(z_{n\alpha})\right] \,, \tag{58a}$$

$$X_{\alpha n}(q,q';-B_3) = -\sqrt{2} m_n \left[\frac{A}{A+1}\frac{1}{q}\,\mathrm{Q}_0(z_{\alpha n}) + \frac{1}{q'}\,\mathrm{Q}_1(z_{\alpha n})\right] \,, \tag{58b}$$

$$X_{nn}(q,q';-B_3) = A\, m_n \left[\frac{A^2+2A+3}{(A+1)^2}\,\mathrm{Q}_0(z_{nn}) + \frac{2}{A+1}\frac{q^2+q'^2}{qq'}\,\mathrm{Q}_1(z_{nn}) + \mathrm{Q}_2(z_{nn})\right] \,, \tag{58c}$$

where Q_l are the Legendre functions of the second kind, which are related the ordinary Legendre Polynomials P_l by

$$\mathrm{Q}_l(z) = \frac{1}{2}\int_{-1}^{1} dx\, \frac{\mathrm{P}_l(x)}{z-x} \tag{59}$$

for $|z|>1$. The arguments $z_{n\alpha}$, $z_{\alpha n}$ and z_{nn} in Eq. (58) are defined as

$$z_{n\alpha} = -\frac{1}{qq'}\left(m_n B_3 + q^2 + \frac{A+1}{2A}q'^2\right) \,, \tag{60a}$$

$$z_{\alpha n} = -\frac{1}{qq'}\left(m_n B_3 + \frac{A+1}{2A}q^2 + q'^2\right) \,, \tag{60b}$$

$$z_{nn} = -\frac{A}{qq'}\left(m_n B_3 + \frac{A+1}{2A}(q^2+q'^2)\right) \,. \tag{60c}$$

In our bound-state situation, $B_3>0$, these three arguments all satisfy the condition $z<-1$.

By inserting Eq. (53a) into (53b), we obtain a single-channel integral equation that includes only the Faddeev component F_n:

$$\begin{aligned} F_n(q) =& 4\pi \int_0^\Lambda q'^2 dq'\, X_{nn}(q,q';-B_3)\,\tau_n(q';-B_3)\,F_n(q') \\ &+ 8\pi \int_0^\Lambda q'^2 dq' \left[4\pi \int_0^\Lambda q''^2 dq''\, X_{n\alpha}(q,q'';-B_3)\,\tau_\alpha(q'';-B_3) X_{\alpha n}(q'',q';-B_3)\right]\tau_n(q';-B_3)\,F_n(q') \,. \end{aligned} \tag{61}$$

Eq. (61) can be diagrammatically expressed in Fig. 3. The last term in Fig. 3 contains two loops, which corresponds to the double integral in Eq. (61). For future reference we define the integral inside the square brackets in Eq. (61) as the function

$$I_{n\alpha n}(q,q';B_3) = 4\pi \int_0^\Lambda q''^2 dq''\, X_{n\alpha}(q,q'';-B_3)\,\tau_\alpha(q'';-B_3) X_{\alpha n}(q'',q';-B_3)\ . \tag{62}$$

Eq. (61) foregrounds a possible inconsistency in our approach. In the Halo EFT power counting both X_{nn} and $I_{n\alpha n}$ are of order Q^0. Meanwhile, in the power counting of Ref. [39] the propagator τ_n scales as $M_{hi}^{-1}Q^{-2}$ (see Eq. (56)). It follows that each iterate of the integral equation (term in the Neumann series [61]) is suppressed by one power of Q/M_{hi} compared to the previous one. If the theory is properly renormalized in the three-body sector, i.e. only momenta of order M_{lo} contribute to the loop integrations, our power counting then leads to the conclusion that there are no ^{6}He bound states. An alternative way to state this is that the power counting of Ref. [39] predicts that the eigenvalues of the integral-equation kernel are of order M_{lo}/M_{hi}, and so there are no solutions to Eq. (61)—provided it is properly renormalized.

Clearly this conclusion is not correct, since ^{6}He exists. The power counting of Ref. [38], which is less "natural" in the $n\alpha$ sector (see Sec. V), does not produce this dilemma in the three-body sector. In that power counting $\tau_n \sim M_{lo}^{-1}Q^{-2}$, and all terms in the Neumann series are of the same size for $Q \sim M_{lo}$. But, in the power counting of Ref. [38], Eq. (56) must also be modified, since the unitarity piece of the $n\alpha$ amplitude is present already at leading order. The corresponding calculation for ^{6}He was carried out in Ref. [43].

C. Renormalization of the ^{6}He ground state

The conclusion of perturbativity also rests on the assumption that Eq. (61) is already renormalized. We now show that this is not the case.

By using a hard cutoff Λ to regularize the integrals of Eqs. (53a, 53b), we obtain B_3 as a function of Λ. This cutoff dependence is illustrated in Fig. 2, which shows that B_3 behaves approximately as Λ^3 at values of Λ that are large compared to k_R, γ_0, and $\sqrt{2m_nB_3}$.

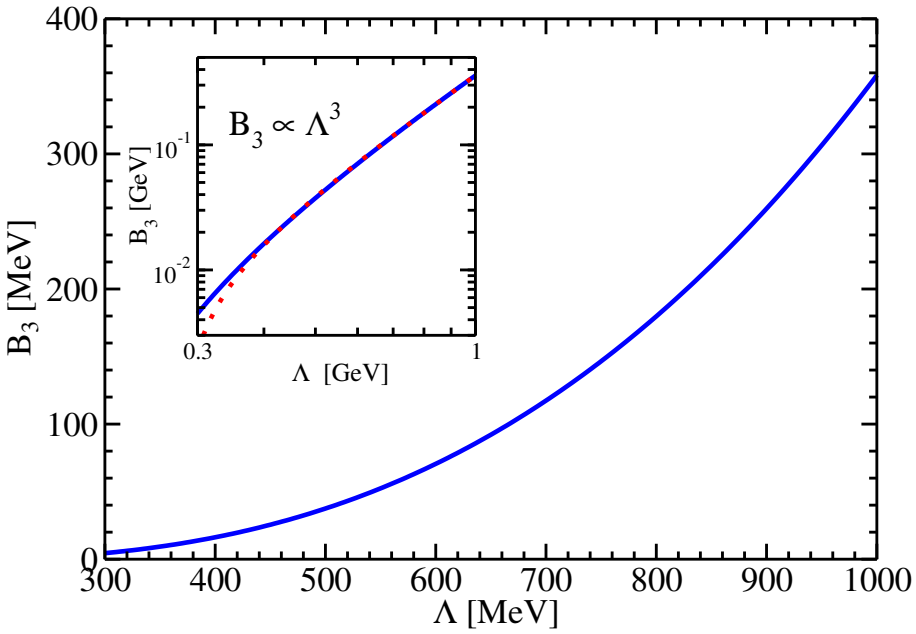

FIG. 2. (Color online) The ^{6}He two-neutron separation energy B_3 as a function of the cutoff Λ. The calculation is based on only two-body interactions. The inner panel compares the numerical result (blue solid line) with a polynomial approximation (red dotted line): $B_3/\mathrm{GeV} = -0.00765 + 0.366(\Lambda/\mathrm{GeV})^3$.

To understand this phenomenon we examine the properties of the kernel of Eq. (61). Since the analytic form of each term in Eq. (62) is already derived, we can calculate the cutoff dependence of $I_{n\alpha n}$ analytically. In fact, the dominant Λ-dependent part of $I_{n\alpha n}$ is proportional to $m_n q q'/\Lambda^2$, and vanishes in the limit $\Lambda \to \infty$. Since X_{nn} is not cutoff

dependent, the kernel of the single-channel integral equation, Eq. (61), is independent of Λ for $\Lambda \gg \sqrt{2m_n B_3}, \gamma_0, k_R$. Thus, the cutoff dependence that appears in Fig. 2 must arise from the solution of the integral equation.

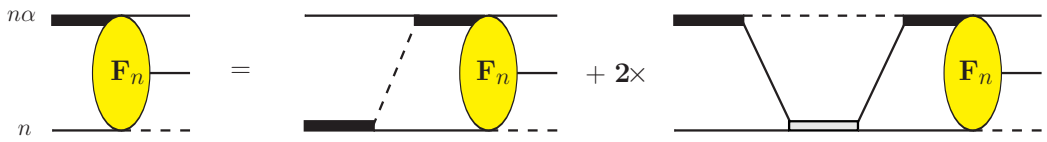

FIG. 3. (Color online) The single-channel Faddeev equation for the ^{6}He bound state. The Faddeev component F_n is solved as integral equation containing a two-loop diagram.

In order to cancel this cutoff dependence, a three-body $nn\alpha$ counterterm is added to the integral equation. A natural choice of this counterterm is one that has the same behavior as the cutoff-dependent piece of $I_{n\alpha n}$, i.e. proportional to $m_n qq'/\Lambda^2$. The dependence on both q and q' indicates the existence of p-wave channels on both sides of the counterterm. Therefore, we introduce a $nn\alpha$ counterterm with a neutron as the spectator on both sides of the counterterm. Choosing a $nn\alpha$ counterterm of this p-wave type is also consistent with the Pauli exclusion principle. The resulting integral equation with the addition of a $nn\alpha$ counterterm is diagrammatically illustrated in Fig. 4.

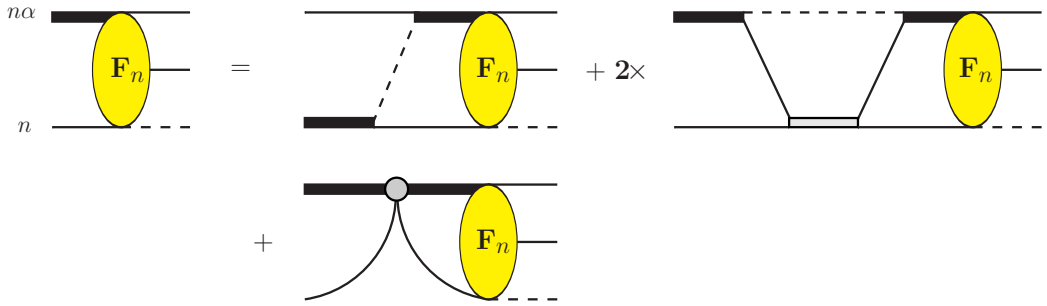

FIG. 4. (Color online) The single-channel Faddeev equation for the ^{6}He bound state with the addition of a $nn\alpha$ counterterm. Both sides of the counterterm are in the spectator-n partition.

In order to include this $nn\alpha$ counterterm, Eq. (61) needs to be modified by adding the following term to the kernel function X_{nn},

$$X_{nn}(q,q';-B_3) \to X_{nn}(q,q';-B_3) - m_n \frac{qq'}{\Lambda^2} H_0(\Lambda) \ , \tag{63}$$

where the minus sign in Eq. (63) is introduced due to the presence of the permutation operator $-\mathcal{P}_{nn}$ in the kernel function X_{nn}. Since $H_0(\Lambda)$ is itself unchanged under the permutation, applying $-\mathcal{P}_{nn}$ to the three-body force will lead to a factor of -1.

By tuning the counterterm parameter $H_0(\Lambda)$, we can cancel the cutoff dependence in the integral equation, Eq. (61), and reproduce the ^{6}He ground-state two-neutron separation energy $B_3 = 0.975$ MeV for all values of Λ. In Fig. 5 we plot the $H_0(\Lambda)$ that is necessary to do this as a function of Λ. It has an oscillatory behavior in $\log\Lambda$—similar to the three-body force's behavior in the leading-order three-boson problem [19]. However, in contrast to the three-boson case, the period of $H_0(\Lambda)$ in $\log\Lambda$ decreases as Λ increases. This difference in the behavior of H_0 may well arise from the $n\alpha$ p-wave interaction in the ^{6}He system: the symmetry of discrete scale invariance, present in three-body systems with resonant s-wave interactions, is broken by this p-wave interaction (cf. [44] which considers a three-body system with all p-wave interactions, and in a zero-range limit different to that discussed here).

After the renormalization, we calculated the Faddeev component $F_n(q)$ from Eq. (61). By inserting the renormalized $F_n(q)$ into the integrals in Eq. (53a), we can calculate $F_\alpha(q)$ without adding an additional counterterm. Fig. 6 shows the Faddeev components F_α and F_n as functions of the momentum q for different values of Λ. The cutoff dependence of the low-q part of both $F_\alpha(q)$ and $F_n(q)$ is weak for $\Lambda > 200$ MeV.

The integral equation (61), modified according to Eq. (63), is now renormalized. And it generates a shallow bound state, with characteristic momenta $\sim M_{lo}$. This seems to contradict the power-counting arguments at the end of the previous subsection. It could be, though, that the binding arises mainly because of short-distance ($\sim 1/M_{hi}$) physics in this EFT, i.e. the "long-range" ($\sim 1/M_{lo}$) effects of X_{nn} and $I_{n\alpha n}$ are perturbative corrections to a fine-tuned ^{5}He-n bound state. Whether or not that is the case warrants further investigation. The calculation we have performed

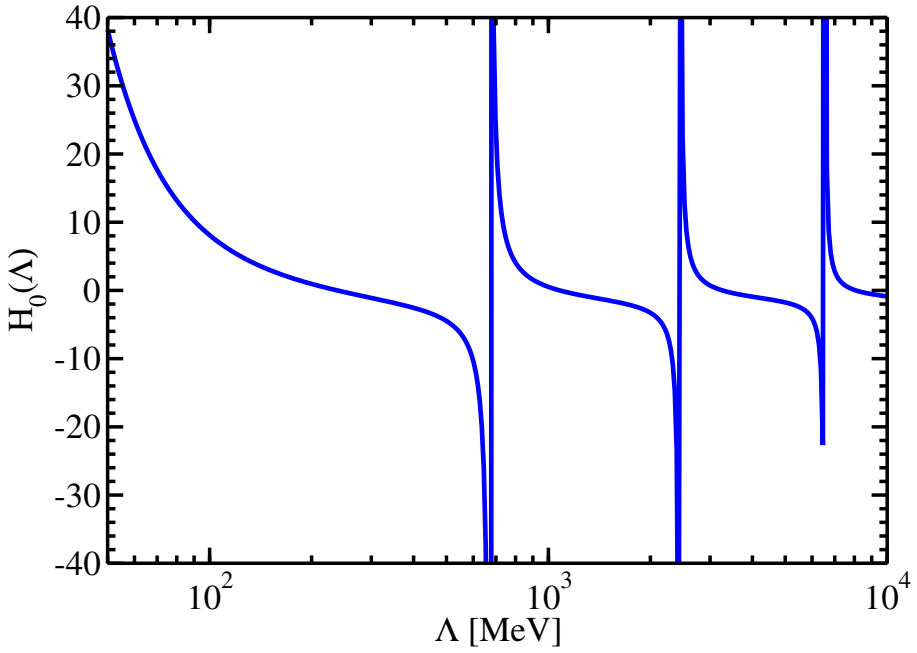

FIG. 5. (Color online) The $nn\alpha$-counterterm parameter H_0 as a function of the cutoff Λ. H_0 is tuned to reproduce $B_3 = 0.975$ MeV at different values of Λ.

here, which only looks at one observable, B_3, cannot definitively decide the issue. We are presently examining the correlations between different observables, such as the charge and matter radii of ^{6}He, calculated with the Faddeev components shown in Fig. 6 [62]. The extent to which X_{nn} and $I_{n\alpha n}$ drive those correlations will help establish whether the power counting of Ref. [39] applies in this system.

Here we have shown the cutoff independence of Faddeev components after renormalization (see Fig. 6). This indicates that one three-body parameter (e.g. B_3) is needed for renormalization of the LO equations that describe ^{6}He in this EFT. In fact, alternative renormalization approaches, e.g. by adding a different three-body counterterm, may be possible. However, any alternative renormalization method must be equivalent to the method used above up to higher-order corrections. The number of three-body renormalization parameters needed for renormalization at LO should not change.

V. SUMMARY AND OUTLOOK

We describe the ^{6}He ground state as a $nn\alpha$ three-body system in the framework of Halo EFT. The two-body, i.e. nn and $n\alpha$, interactions are expanded under an EFT power counting that produces—at leading order (LO)—the narrow p-wave resonance in the $n\alpha$ $^2\mathrm{P}_{3/2}$ channel and the virtual state in the $^1\mathrm{S}_0$ channel of nn scattering. These nn and $n\alpha$ t-matrices are implemented in our LO analysis of the ^{6}He ground state, which employs a Faddeev formulation to calculate the ^{6}He two-neutron separation energy, B_3, as well as the Faddeev components, F_α and F_n, via two coupled integral equations. The result for the ^{6}He two-neutron separation energy is strongly cutoff dependent. To remedy this we introduce a p-wave $nn\alpha$ counterterm and perform a renormalization in the three-body 0^+ sector of the theory. By tuning the parameter H_0 of the three-body counterterm, we can reproduce the experimental value of $B_3 = 0.975$ MeV. The bound-state Faddeev components F_α and F_n are then predicted, and they are both cutoff independent.

The parameter H_0 is studied as a function of the cutoff. It exhibits a log-periodic behavior with decreasing periods at large cutoffs. A similar log-periodicity of the three-body-counterterm parameter, however with a constant period, has been observed in the leading-order calculation of three-body systems with s-wave interactions. The different large-Λ behavior could be caused by properties of the p-wave $n\alpha$ interactions in the ^{6}He system, which breaks the scale-invariance symmetry that is present at LO in the three-body system with only s-wave interactions.

The Halo EFT for ^{6}He presented here bears a significant similarity to cluster models. For example, in Refs. [14, 15] Ghovanlou and Lehman used separable Yamaguchi potentials for the nn and $n\alpha$ interactions. They fitted the parameters to known phase-shifts in these systems and then predicted the binding energy of ^{6}He, ultimately obtaining a value smaller than that seen in experiment. In fact, two-body phase-shifts are insufficient to determine the three-

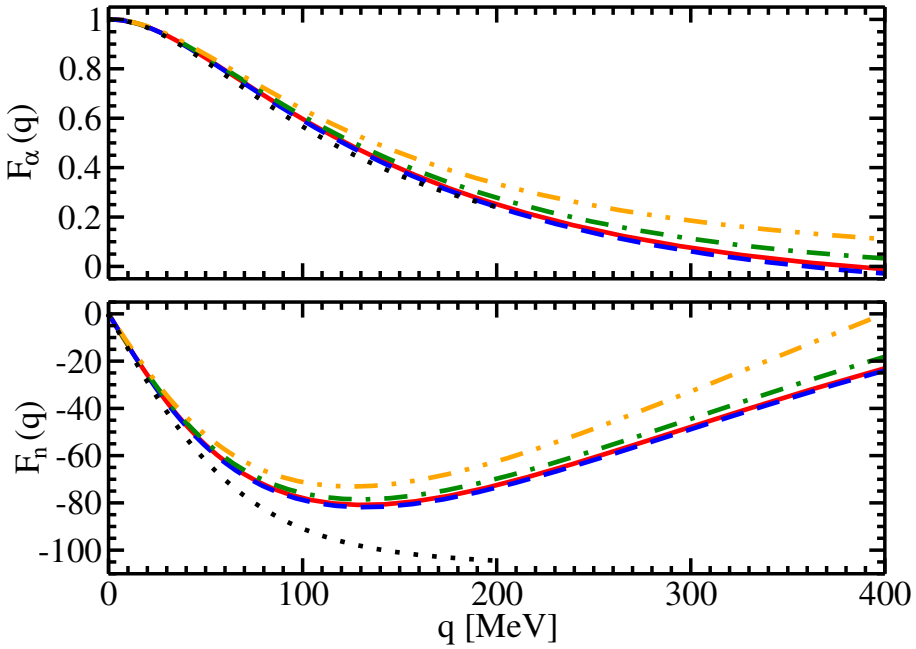

FIG. 6. (Color online) The Faddeev components F_α and F_n as functions of q, calculated with cutoff parameters Λ at 200 MeV (black dotted line), 400 MeV (orange dot-dot-dashed line), 800 MeV (green dot-dashed line), 1.6 GeV (blue dashed line) and 3.2 GeV (red solid line). The Faddeev components are normalized to provide $F_\alpha(0) = 1$.

body binding energy in these systems. This fact is reflected in the EFT calculation by the sensitivity to the cutoff parameter. The EFT then mandates the introduction of a three-body parameter at LO, and ultimately this may be a more effective path to a cluster description of the ^{6}He nucleus than one based on two-body potentials alone.

Of course, there are higher-order corrections in the EFT, which will perturb the result obtained here. These include the effective-range terms in the nn-^{1}S$_0$ channel and higher-order effects in the $n\alpha$-^{2}P$_{3/2}$ channel, the role of the $n\alpha$-^{2}S$_{1/2}$ and ^{2}P$_{1/2}$ channels, etc. These will be investigated in future work. These higher-order terms can be studied perturbatively using methods similar to those of Refs. [57–60]. The power counting of Ref. [39] indicates that the expansion parameter of the EFT is $M_{lo}/M_{hi} \sim 1/4$, which is similar to the one for the "pionless" EFT that has been applied with much success to few-nucleon systems. However, success there was achieved only after higher-order corrections were included in the analysis, To compare with experimental measurements in these systems at a high accuracy, higher-order effects must be included in the EFT calculation.

In the renormalization of the $n\alpha$ interaction, we adopt the power counting by Bedaque *et al.* [39], i.e. $a_1 \sim M_{lo}^{-2}M_{hi}^{-1}$ and $r_1 \sim M_{hi}$, to extract the corresponding p-wave resonance. An alternative power counting is introduced by Bertulani *et al.* [38] for studying the $n\alpha$ p-wave interaction. In that work $a_1 \sim M_{lo}^{-3}$ and $r_1 \sim M_{lo}$. Therefore, both γ_1 and $k_\pm$ are of order M_{lo}, which means both a shallow bound state and a low-energy resonance are present. This result to some extent contradicts the experimentally known absence of the ^{5}He bound state. Meanwhile, in contrast to the power counting in Ref. [39], which requires one fine-tuning in the renormalization, the power counting in [38] requires two fine-tunings, which is less "natural". It was this power counting that was used by Rotureau and van Kolck in their calculations of ^{6}He ground state [43].

In that study the authors solved for the Helium-6 bound state using the Gamow shell-model basis. As we did, they introduced a p-wave $nn\alpha$ counterterm in order to render their results independent of the ultraviolet cutoff on the shell-model basis. However, the corresponding three-body parameter vanishes in the limit $\Lambda \to \infty$, and does not appear to oscillate as a function of Λ. It thus behaves differently from our three-body parameter. Presumably this is a result of the different power counting used for the $n\alpha$ interaction, which leads to different ultraviolet behavior of the integral-equation kernel. This deserves further investigation.

Our work and Ref. [43] both reproduce the experimental value of ^{6}He two-neutron separation energy. A comparison of the different power counting schemes for ^{6}He can be achieved if other physical observables in the ^{6}He system can be predicted. In our approach, the Faddeev components, F_α and F_n, are calculated after the renormalization, and are therefore a prediction. Using F_α and F_n, we will be able to construct the ^{6}He wave function and from it the matter-density form factors. These form factors can be used to obtain predictions for the mean square radii (cf. Ref. [10]) and other observables. The calculation of these quantities is in progress [62]. The accuracy of the

LO Halo-EFT description can also be assessed by examining properties of the $nn\alpha$ system in the continuum. The low-energy $nn\alpha$ continuum was investigated in, e.g. Refs. [63] within a cluster description, as well as in Refs. [64, 65] via *ab initio* calculations. The Faddeev formalism developed here can be readily extended to continuum states and used to compute, e.g. LO Halo-EFT predictions for the resonance-pole positions of excited states in the ^{6}He system.

In our calculations, the neutron-core mass ratio is kept as a variable (A). This opens up a possible extensions of the current ^{6}He analysis to other p-wave halo nuclei with a different neutron-core mass ratio. One important example is the ^{11}Li nucleus, which is another Borromean system but with a $\frac{3}{2}^-$ ground state. A recent measurement of the two-neutron transfer reaction, ^{1}H(^{11}Li,^{9}Li)^{3}H, at the ISAC-II facility at TRIUMF, implies that both the s- and p-wave components of $n-^9$Li interactions contribute significantly to the ground-state ^{11}Li [66]. This suggests that a LO EFT analysis of the ^{11}Li nucleus should include both the s- and p-wave $n-^9$Li interactions non-perturbatively (cf. Ref. [27]), yielding a Faddeev equation that includes more channels than does that for ^{6}He at LO. But, similarly to ^{6}He, we can also calculate the binding energy and matter radius in ^{11}Li. In the case of ^{11}Li it will be important to understand whether the presence of additional channels in the LO calculation means that more than one three-body parameter is needed for renormalization at LO.

ACKNOWLEDGMENTS

This work was supported by the U.S. Department of Energy under grant DE-FG02-93ER40756 and also in part by both the Natural Sciences and Engineering Research Council (NSERC) and the National Research Council of Canada. We thank the Institute for Nuclear Theory at the University of Washington for its hospitality during the program INT-14-1 "Universality in Few-Body Systems" when the work was finalized. We are indebted to Lucas Platter, Arbin Thapaliya, Bira van Kolck and Gerry Hale for useful discussions.

Appendix A: Renormalization with Yamaguchi form factors

Choosing the form factor $g_l(q)$ present in Eq. (20) of Yamaguchi form (23), and assuming $\beta_l \sim M_{hi}$, we can regularize Eq. (22) to express τ_l's dependence on M_{hi}. The two-body coupling constant λ_l is then tuned correspondingly to cancel this divergence. By doing so, we can reproduce the low-energy behavior of the two-body t-matrices of Eqs. (5, 8).

For s-wave scattering, $l = 0$, we have

$$\begin{aligned}\tau_0^{-1}(E) =&\frac{1}{\lambda_0} + 8\pi\mu \int_0^\infty dq\, \frac{q^2\beta_0^4}{(q^2 - k^2 - i\epsilon)(q^2+\beta_0^2)^2}\\ =&\frac{1}{\lambda_0} + 2\pi^2\mu\frac{\beta_0^3}{(\beta_0 - ik)^2}\ .\end{aligned} \tag{A1}$$

We substitute $\tau_0(E)$ of Eq. (A1) and $g_0(k)$ of Eq. (23) into Eq. (21), and expand the resulting nn scattering t-matrix in powers of k/β_0 and obtain

$$\begin{aligned}\langle \boldsymbol{k}|t_{nn}|\boldsymbol{k'}\rangle =&g_0^2(k)\,\tau_0(E)\\ =&\left(1+\frac{k^2}{\beta_0^2}\right)^{-2}\left[\frac{1}{\lambda_0} + 2\pi^2\mu_{nn}\beta_0\left(1 + i\frac{k}{\beta_0} - \frac{k^2}{\beta_0^2} + \cdots\right)^2\right]^{-1}\\ =&\frac{1}{4\pi^2\mu_{nn}}\left\{\left(\frac{\beta_0}{2} + \frac{1}{4\pi^2\mu_{nn}\lambda_0}\right) - \left[\frac{3}{2\beta_0} - \frac{2}{\beta_0^2}\left(\frac{\beta_0}{2} + \frac{1}{4\pi^2\mu_{nn}\lambda_0}\right)\right]k^2 + ik\right\}^{-1}\ .\end{aligned} \tag{A2}$$

By tuning both β_0 and λ_0, a_0 and r_0 are reproduced in the renormalization as

$$\frac{1}{a_0} =\frac{\beta_0}{2} + \frac{1}{4\pi^2\mu_{nn}\lambda_0}\ , \tag{A3a}$$

$$\frac{r_0}{2} =\frac{3}{2\beta_0} - \frac{2}{\beta_0^2}\frac{1}{a_0}\ . \tag{A3b}$$

Note that since $\beta_0 \sim M_{hi}$, if λ_0 is fine tuned in renormalization so that $1/a_0 \sim M_{lo}$, then $r_0 \sim 1/M_{hi}$ will be naturally obtained.

For the p-wave interaction $l=1$ we calculate τ_1 from Eq. (22) as

$$\begin{aligned}\tau_1^{-1}(E) =&\frac{1}{\lambda_1}+8\pi\mu\int_0^\infty dq\,\frac{q^4\beta_1^8}{(q^2-k^2-i\epsilon)(q^2+\beta_1^2)^4}\\ =&\frac{1}{\lambda_1}+\frac{\pi^2\mu}{4}\beta_1^5\,\frac{\beta_1^2-4i\beta_1 k-k^2}{(\beta_1-ik)^4}\ .\end{aligned}\tag{A4}$$

We expand $g_1(k)$ and $\tau_1(E)$ in powers of k, substitute them into Eq. (21), and then obtain the $n\alpha$ scattering t-matrix as

$$\begin{aligned}\langle\boldsymbol{k}|t_{n\alpha}|\boldsymbol{k'}\rangle =&3\hat{\boldsymbol{k}}\cdot\hat{\boldsymbol{k}}'\,g_1^2(k)\,\tau_1(E)\\ =&3\boldsymbol{k}\cdot\boldsymbol{k'}\left(1+\frac{k^2}{\beta_1^2}\right)^{-4}\left[\frac{1}{\lambda_1}+\frac{\pi^2\mu_{n\alpha}}{4}\beta_1^3\,\left(1-i\frac{4k}{\beta_1}-\frac{k^2}{\beta_1^2}\right)\left(1+\frac{ik}{\beta_1}-\frac{k^2}{\beta_1^2}+\cdots\right)^4\right]^{-1}\\ =&\frac{3\boldsymbol{k}\cdot\boldsymbol{k'}}{4\pi^2\mu_{n\alpha}}\left\{\left(\frac{\beta_1^3}{16}+\frac{1}{4\pi^2\mu_{n\alpha}\lambda_1}\right)+\left[\frac{5\beta_1}{16}+\frac{4}{\beta_1^2}\left(\frac{\beta_1^3}{16}+\frac{1}{4\pi^2\mu_{n\alpha}\lambda_1}\right)\right]k^2+ik^3\right\}^{-1}.\end{aligned}\tag{A5}$$

In the p-wave renormalization, a_1 and r_1 can be reproduced from the relation

$$\frac{1}{a_1}=\frac{\beta_1^3}{16}+\frac{1}{4\pi^2\mu_{n\alpha}\lambda_1}\ ,\tag{A6a}$$

$$\frac{r_1}{2}=-\frac{5\beta_1}{16}-\frac{4}{\beta_1^2}\frac{1}{a_1}\ .\tag{A6b}$$

Note that since $\beta_1\sim M_{hi}$, if λ_1 is tuned so that $1/a_1\sim M_{lo}^2M_{hi}$, then we can naturally have $r_1\sim M_{hi}$.

Appendix B: The Kernel Functions $X_{n\alpha}$, $X_{\alpha n}$ and X_{nn}

1. The spin–and–orbital-angular-momentum decomposition

The spin matrix elements between different spectator representations can be calculated using Wigner's 6-j symbol:

$$\langle s_1,(s_2s_3)s_{23};S|\ (s_1s_2)s_{12},s_3;S\rangle=(-1)^{s_1+s_2+s_3+S}\sqrt{(2s_{12}+1)(2s_{23}+1)}\begin{Bmatrix}s_1 & s_2 & s_{12}\\ s_3 & S & s_{23}\end{Bmatrix}\ .\tag{B1}$$

Therefore, in ^{6}He's ground state, the spin matrix elements between states represented in either n- or α-spectator representations are calculated as

$${}_\alpha\left\langle\left(\frac{1}{2}\,\frac{1}{2}\right)0,0;S_\alpha=0,M_{S\alpha}=0\,\middle|\,\left(\frac{1}{2}0\right)\frac{1}{2},\frac{1}{2};\,S_n=L_n,M_{Sn}=-M_{Ln}\right\rangle_n=-\delta_{0,L_n}\delta_{0,M_{Ln}}\ ,\tag{B2a}$$

$${}_n\left\langle\left(\frac{1}{2}0\right)\frac{1}{2},\frac{1}{2};\,S_n=L_n,M_{Sn}=-M_{Ln}\,\middle|\,\left(\frac{1}{2}\,\frac{1}{2}\right)0,0;S_\alpha=0,M_{S\alpha}=0\right\rangle_\alpha=-\delta_{0,L_n}\delta_{0,M_{Ln}}\ ,\tag{B2b}$$

$$\begin{aligned}{}_n\left\langle\left(\frac{1}{2}0\right)\frac{1}{2},\frac{1}{2};\,S_n=L_n,M_{Sn}=-M_{Ln}\,\middle|\,\mathcal{P}_{nn}\,\middle|\left(\frac{1}{2}0\right)\frac{1}{2},\frac{1}{2};\,S_n=L_n',M_{Sn}=-M_{Ln'}\right\rangle_n\\ =(-1)^{1-L_n}\delta_{L_n,L_n'}\,\delta_{M_{Ln},M_{Ln'}}\ .\end{aligned}\tag{B2c}$$

By substituting Eqs. (B2) into Eqs. (36, 37), we can decompose the spin and orbital-angular-momentum parts of the matrix elements ${}_i\langle p,q;\Omega_i|p',q';\Omega_j\rangle_j$ in the ^{6}He system as

$${}_\alpha\langle p,q;\Omega_\alpha|p',q';\Omega_n\rangle_n=-\sqrt{\frac{2}{3}}\ {}_\alpha\langle p,q;\ 0,0;L_\alpha=M_{L\alpha}=0|p',q';\ 1,1;\ L_n=M_{Ln}=0\rangle_n\ ,\tag{B3a}$$

$${}_n\langle p,q;\Omega_n|p',q';\Omega_\alpha\rangle_\alpha=-\sqrt{\frac{2}{3}}\ {}_n\langle p,q;\ 0,0;L_n=M_{Ln}=0|p',q';\ 1,1;\ L_\alpha=M_{L\alpha}=0\rangle_\alpha\ ,\tag{B3b}$$

$${}_n\langle p,q;\Omega_n|-\mathcal{P}_{nn}|p',q';\Omega_n\rangle_n=\sum_{L_n=0}^{1}\sum_{M_{Ln}=-L_n}^{L_n}\frac{(-2)^{1-L_n}}{6L_n+3}\,{}_n\langle p,q;\ 0,0;L_n,M_{Ln}|-\mathcal{P}_{nn}|p',q';\ 1,1;\ L_n,M_{Ln}\rangle_n\ .\tag{B3c}$$

Inserting Eqs. (B3) into Eq. (49), we can decouple the Kernel functions, X_{ij}, in the ^{6}He problem into a summation of functions $\mathcal{Z}_{ij}^{(L)}$ at different overall orbital angular momentum L:

$$X_{\alpha n}(q,q';E) = -\sqrt{\frac{2}{3}}\mathcal{Z}_{\alpha n}^{(0)}(q,q';E)\ , \tag{B4a}$$

$$X_{n\alpha}(q,q';E) = -\sqrt{\frac{2}{3}}\mathcal{Z}_{n\alpha}^{(0)}(q,q';E)\ , \tag{B4b}$$

$$X_{nn}(q,q';E) = -\frac{2}{3}\mathcal{Z}_{nn}^{(0)}(q,q';E) + \frac{1}{3}\mathcal{Z}_{nn}^{(1)}(q,q';E)\ . \tag{B4c}$$

In the spectator-α representation $L=0$; while in the spectator-n representation L can be zero or one. Those functions $\mathcal{Z}_{ij}^{(L)}$ are then

$$\mathcal{Z}_{\alpha n}^{(0)}(q,q';E) = \iint p^2dp\,p'^2dp'\,g_0(p)G_0^{(\alpha)}(p,q;E)\,g_1(p')\,{}_\alpha\langle p,q;\,(00)00\,|\,p',q';\,(11)00\rangle_n\ , \tag{B5a}$$

$$\mathcal{Z}_{n\alpha}^{(0)}(q,q';E) = \iint p^2dp\,p'^2dp'\,g_1(p)G_0^{(n)}(p,q;E)\,g_0(p')\,{}_n\langle p,q;\,(11)00\,|\,p',q';\,(00)00\rangle_\alpha\ , \tag{B5b}$$

$$\mathcal{Z}_{nn}^{(L)}(q,q';E) = \iint p^2dp\,p'^2dp'\,g_1(p)G_0^{(n)}(p,q;E)\,g_1(p')\,{}_n\langle p,q;\,(11)LM\,|-\mathcal{P}_{nn}|\,p',q';\,(11)LM\rangle_n\ . \tag{B5c}$$

$\mathcal{Z}_{nn}^{(L)}$ is independent of the quantum number M for both the $L=0$ and $L=1$ cases, which will be proved later.

2. The Funcions $\mathcal{Z}_{\alpha n}^{(0)}$, $\mathcal{Z}_{n\alpha}^{(0)}$ and $\mathcal{Z}_{nn}^{(L)}$

Here we we calculate the orbital-angular-momentum–dependent kernel functions $\mathcal{Z}_{\alpha n}^{(0)}$, $\mathcal{Z}_{n\alpha}^{(0)}$ and $\mathcal{Z}_{nn}^{(L)}$.

a. The Function $\mathcal{Z}_{\alpha n}^{(0)}$

After inserting two complete sets of Jacobi-momentum states, we can write $\mathcal{Z}_{\alpha n}^{(0)}$ as

$$\begin{aligned}\mathcal{Z}_{\alpha n}^{(0)}(q,q';E) = &\iint p^2dp\,p'^2dp'\,g_0(p)G_0^{(\alpha)}(p,q;E)\,g_1(p')\iint d^3p_1d^3q_1\iint d^3p_2d^3q_2\\ &\times\ {}_\alpha\langle p,q;\,(00)00\,|\boldsymbol{p_1q_1}\rangle_\alpha\,{}_\alpha\langle\boldsymbol{p_1q_1}|\boldsymbol{p_2q_2}\rangle_n\,{}_n\langle\boldsymbol{p_2q_2}|\,p',q';\,(11)00\rangle_n\ ,\end{aligned} \tag{B6}$$

where the matrix elements containing the orbital-angular-momentum quantum numbers can be expressed as

$${}_\alpha\langle\boldsymbol{p_1q_1}|p,q;\,(00)00\rangle_\alpha = \frac{1}{p_1^2}\delta(p_1-p)\frac{1}{q_1^2}\delta(q_1-q)\mathcal{Y}_{00}^{00}(\hat{\boldsymbol{p}}_1\hat{\boldsymbol{q}}_1)\ , \tag{B7a}$$

$${}_n\langle\boldsymbol{p_2q_2}|p',q';\,(11)00\rangle_n = \frac{1}{p_2^2}\delta(p_2-p')\frac{1}{q_2^2}\delta(q_2-q')\mathcal{Y}_{11}^{00}(\hat{\boldsymbol{p}}_2\hat{\boldsymbol{q}}_2)\ . \tag{B7b}$$

The function $\mathcal{Y}_{l_1l_2}^{LM}$ indicates the orbital-angular-momentum coupling of two spherical harmonics to produce an overall orbital angular momentum L and z-component M:

$$\mathcal{Y}_{l_1l_2}^{LM}(\hat{\boldsymbol{q}}_1\hat{\boldsymbol{q}}_2) = \sum_{m_1m_2} C(l_1l_2L|m_1m_2M)\,\mathrm{Y}_{l_1m_1}(\hat{\boldsymbol{q}}_1)\,\mathrm{Y}_{l_2m_2}(\hat{\boldsymbol{q}}_2)\ . \tag{B8}$$

Also, the transition between the free momentum states $|\boldsymbol{p_1q_1}\rangle_\alpha$ and $|\boldsymbol{p_2q_2}\rangle_n$ yields the product of two delta functions:

$${}_\alpha\langle\boldsymbol{p_1q_1}|\boldsymbol{p_2q_2}\rangle_n = \delta^{(3)}(\boldsymbol{p}_1-\boldsymbol{P}_{\alpha n})\delta^{(3)}(\boldsymbol{p}_2+\boldsymbol{P'}_{\alpha n})\ , \tag{B9}$$

with

$$\boldsymbol{P}_{\alpha n} = \frac{\mu_{nn}}{m_n}\boldsymbol{q}_1+\boldsymbol{q}_2 = \frac{1}{2}\boldsymbol{q}_1+\boldsymbol{q}_2\ , \tag{B10a}$$

$$\boldsymbol{P'}_{\alpha n} = \boldsymbol{q}_1+\frac{\mu_{n\alpha}}{m_n}\boldsymbol{q}_2 = \boldsymbol{q}_1+\frac{A}{A+1}\boldsymbol{q}_2\ , \tag{B10b}$$

where $q_1 = q$ and $q_2 = q'$ are determined from Eqs. (B7).

By applying Eqs. (B7–B10) into Eq. (B6), we obtain

$$\begin{aligned}\mathcal{Z}^{(0)}_{\alpha n}(q,q';E) =& \int d\hat{\boldsymbol{q}}_1 \int d\hat{\boldsymbol{q}}_2\, g_0(P_{\alpha n}) G^{(\alpha)}_0(P_{\alpha n},q;E)\, g_1(P'_{\alpha n}) \mathcal{Y}^{00\,*}_{00}(\hat{\boldsymbol{P}}_{\alpha n}\hat{\boldsymbol{q}}_1)\, \mathcal{Y}^{00}_{11}(-\hat{\boldsymbol{P}}'_{\alpha n}\,\hat{\boldsymbol{q}}_2) \\ =& \frac{1}{4\pi}\int d\hat{\boldsymbol{q}}_1 \int d\hat{\boldsymbol{q}}_2\, g_0(P_{\alpha n}) G^{(\alpha)}_0(P_{\alpha n},q;E)\, g_1(P'_{\alpha n}) \sum_{m=-1}^{1} C(110|m\,-m\,0) \mathrm{Y}_{1m}(-\hat{\boldsymbol{P}}'_{\alpha n})\, \mathrm{Y}_{1-m}(\hat{\boldsymbol{q}}_2)\ ,\end{aligned} \tag{B11}$$

where we used the fact that $\mathcal{Y}^{00}_{00}(\hat{\boldsymbol{P}}_{\alpha n}\hat{\boldsymbol{q}}_1) = 1/(4\pi)$.

Using the relation [54]

$$\mathrm{Y}_{lm}(\widehat{\boldsymbol{r_1}+\boldsymbol{r_2}}) = \sum_{l_1+l_2=l} \sqrt{\frac{4\pi\,(2l+1)!}{(2l_1+1)!\,(2l_2+1)!}}\, \frac{r_1^{l_1} r_2^{l_2}}{|\boldsymbol{r_1}+\boldsymbol{r_2}|^l} \sum_{m_1 m_2} C(l_1 l_2 l|m_1 m_2 m)\, \mathrm{Y}_{l_1 m_1}(\hat{\boldsymbol{r}}_1)\, \mathrm{Y}_{l_2 m_2}(\hat{\boldsymbol{r}}_2)\ , \tag{B12}$$

we rewrite Eq. (B11) as

$$\begin{aligned}\mathcal{Z}^{(0)}_{\alpha n}(q,q';E) =& \frac{1}{4\pi}\int d\hat{\boldsymbol{q}}_1 \int d\hat{\boldsymbol{q}}_2\, g_0(P_{\alpha n}) G^{(\alpha)}_0(P_{\alpha n},q;E)\, g_1(P'_{\alpha n})\, P'^{\,l-1}_{\alpha n} \\ & \times \sum_{m=-1}^{1} C(110|m\,-m\,0) \sum_{l_1+l_2=1} \sqrt{\frac{4\pi\,3!}{(2l_1+1)!\,(2l_2+1)!}}\, q^{l_1} \left(\frac{A}{A+1}q'\right)^{l_2} \\ & \times \sum_{m_1 m_2} C(l_1 l_2 1|m_1 m_2 m) \mathrm{Y}_{l_1 m_1}(-\hat{\boldsymbol{q}}_1)\, \mathrm{Y}_{l_2 m_2}(-\hat{\boldsymbol{q}}_2) \mathrm{Y}_{1-m}(\hat{\boldsymbol{q}}_2)\ .\end{aligned} \tag{B13}$$

We can perform a Legendre expansion of the product of terms in front of the first summation in Eq. (B13). Since the Halo EFT calculation takes $g_0(P_{\alpha n}) = 1$ and $g_1(P'_{\alpha n}) = P'_{\alpha n}$, we have

$$g_0(P_{\alpha n}) G^{(\alpha)}_0(P_{\alpha n},q;E)\, g_1(P'_{\alpha n})\, P'^{\,l-1}_{\alpha n} = G^{(\alpha)}_0(P_{\alpha n},q;E) = 4\pi \sum_{t\nu} \mathcal{G}^t_{\alpha n}(q,q';E)\, \mathrm{Y}^*_{t\nu}(\hat{\boldsymbol{q}}_1) \mathrm{Y}_{t\nu}(\hat{\boldsymbol{q}}_2)\ , \tag{B14}$$

where $\mathcal{G}^t_{\alpha n}$ is determined by

$$\begin{aligned}\mathcal{G}^t_{\alpha n}(q,q';E) =& \frac{1}{2}\int_{-1}^{1} dx\, \mathrm{P}_t(x)\, G^{(\alpha)}_0(P_{\alpha n},q;E) \\ =& \frac{1}{2}\int_{-1}^{1} dx\, \mathrm{P}_t(x) \left[E - \frac{1}{m_n}\left(\frac{1}{4}q^2 + q'^2 + qq'x\right) - \frac{A+2}{4A\,m_n}q^2\right]^{-1} \\ =& \frac{m_n}{2qq'}\int_{-1}^{1} dx\, \mathrm{P}_t(x) \left[\frac{1}{qq'}\left(m_n E - \frac{A+1}{2A}q^2 - q'^2\right) - x\right]^{-1}\ .\end{aligned} \tag{B15}$$

If we define

$$z_{\alpha n} = \frac{1}{qq'}\left(m_n E - \frac{A+1}{2A}q^2 - q'^2\right)\ , \tag{B16}$$

we can relate $\mathcal{G}^t_{\alpha n}(q,q';E)$ to the Legendre functions of the second kind Q_t (see Eq. (59)) as

$$\mathcal{G}^t_{\alpha n}(q,q';E) = \frac{m_n}{qq'}\, \mathrm{Q}_t(z_{\alpha n})\ . \tag{B17}$$

Here we take the opportunity to write explicitly the three Q_l's used in our calculation as

$$\mathrm{Q}_0(z) = \frac{1}{2}\ln\left(\frac{z+1}{z-1}\right) \tag{B18a}$$

$$\mathrm{Q}_1(z) = \frac{1}{2}z\ln\left(\frac{z+1}{z-1}\right) - 1 \tag{B18b}$$

$$\mathrm{Q}_2(z) = \frac{1}{2}\left(-\frac{1}{2} + \frac{3}{2}z^2\right)\ln\left(\frac{z+1}{z-1}\right) - \frac{3}{2}z\ . \tag{B18c}$$

Now the dependences on $\hat{\boldsymbol{q}}_1$ and $\hat{\boldsymbol{q}}_2$ are separated and can be integrated individually as

$$\begin{aligned}\mathcal{Z}^{(0)}_{\alpha n}(q,q';E) =& \sum_t \mathcal{G}^t_{\alpha n}(q,q';E) \sum_{m=-1}^{1} C(110|m\ -m\,0) \sum_{l_1+l_2=1} \sqrt{\frac{4\pi\,3!}{(2l_1+1)!\,(2l_2+1)!}} \\ &\times\ q^{l_1} \left(\frac{A}{A+1}q'\right)^{l_2} \sum_{m_1 m_2} C(l_1 l_2 1|m_1 m_2 m) \\ &\times \sum_{\nu=-t}^{t} \int d\hat{\boldsymbol{q}}_1\, \mathrm{Y}^*_{t\nu}(\hat{\boldsymbol{q}}_1) \mathrm{Y}_{l_1 m_1}(-\hat{\boldsymbol{q}}_1) \int d\hat{\boldsymbol{q}}_2\, \mathrm{Y}_{t\nu}(\hat{\boldsymbol{q}}_2) \mathrm{Y}_{l_2 m_2}(-\hat{\boldsymbol{q}}_2) \mathrm{Y}_{1-m}(\hat{\boldsymbol{q}}_2)\ . \end{aligned} \tag{B19}$$

After integrating the product of spherical harmonics, we sum up all the orbital-angular-momentum quantum numbers using properties of Clebsch-Gordan coefficients (see e.g., in Ref. [67]), and express $\mathcal{Z}^{(0)}_{\alpha n}$ as a summation of $\mathcal{G}^t_{\alpha n}$'s:

$$\mathcal{Z}^{(0)}_{\alpha n}(q,q';E) = \sqrt{3}\left(\frac{A}{A+1}q'\,\mathcal{G}^0_{\alpha n}(q,q';E) + q\,\mathcal{G}^1_{\alpha n}(q,q';E)\right)\ . \tag{B20}$$

b. The Function $\mathcal{Z}^{(0)}_{n\alpha}$

Similarly, $\mathcal{Z}^{(0)}_{n\alpha}$ is calculated as

$$\begin{aligned}\mathcal{Z}^{(0)}_{n\alpha}(q,q';E) =& \iint p^2 dp\, p'^2 dp'\, g_1(p) G^{(n)}_0(p,q;E)\, g_0(p') \iint d^3p_1 d^3q_1 \iint d^3p_2 d^3q_2 \\ &\times\ {}_n\langle p,q;\,(11)00\,|\boldsymbol{p_1 q_1}\rangle_n\, {}_n\langle \boldsymbol{p_1 q_1}|\boldsymbol{p_2 q_2}\rangle_\alpha\, {}_\alpha\langle \boldsymbol{p_2 q_2}|\,p',q';\,(00)00\rangle_\alpha\ . \end{aligned} \tag{B21}$$

We express the orbital-angular-momentum dependent matrix elements as

$${}_n\langle \boldsymbol{p_1 q_1}|p,q;\,(11)00\rangle_n = \frac{1}{p_1^2}\delta(p_1-p)\frac{1}{q_1^2}\delta(q_1-q)\mathcal{Y}^{00}_{11}(\hat{\boldsymbol{p}}_1\hat{\boldsymbol{q}}_1)\ , \tag{B22a}$$

$${}_\alpha\langle \boldsymbol{p_2 q_2}|p',q';\,(00)00\rangle_\alpha = \frac{1}{p_2^2}\delta(p_2-p')\frac{1}{q_2^2}\delta(q_2-q')\mathcal{Y}^{00}_{00}(\hat{\boldsymbol{p}}_2\hat{\boldsymbol{q}}_2)\ . \tag{B22b}$$

Also the transition between momentum states $|\boldsymbol{p_1 q_1}\rangle_n$ and $|\boldsymbol{p_2 q_2}\rangle_\alpha$ yields

$${}_n\langle \boldsymbol{p_1 q_1}|\boldsymbol{p_2 q_2}\rangle_\alpha = \delta^{(3)}(\boldsymbol{p}_1 + \boldsymbol{P}_{n\alpha})\delta^{(3)}(\boldsymbol{p}_2 - \boldsymbol{P'}_{n\alpha})\ , \tag{B23}$$

where

$$\boldsymbol{P}_{n\alpha} = \frac{\mu_{n\alpha}}{m_n}\boldsymbol{q}_1 + \boldsymbol{q}_2 = \frac{A}{A+1}\boldsymbol{q}_1 + \boldsymbol{q}_2\ , \tag{B24a}$$

$$\boldsymbol{P}'_{n\alpha} = \boldsymbol{q}_1 + \frac{\mu_{nn}}{m_n}\boldsymbol{q}_2 = \boldsymbol{q}_1 + \frac{1}{2}\boldsymbol{q}_2\ , \tag{B24b}$$

with $q_1 = q$ and $q_2 = q'$ determined from Eqs. (B22).

Therefore, we can rewrite Eq. (B21) as

$$\mathcal{Z}^{(0)}_{n\alpha}(q,q';E) = \int d\hat{\boldsymbol{q}}_1 \int d\hat{\boldsymbol{q}}_2\, g_1(P_{n\alpha}) G^{(n)}_0(P_{n\alpha},q;E)\, g_0(P'_{n\alpha}) \mathcal{Y}^{00\,*}_{11}(-\hat{\boldsymbol{P}}_{n\alpha}\hat{\boldsymbol{q}}_1)\, \mathcal{Y}^{00}_{00}(\hat{\boldsymbol{P}}'_{n\alpha}\,\hat{\boldsymbol{q}}_2)\ , \tag{B25}$$

where $\mathcal{Y}^{00}_{00}(\hat{\boldsymbol{P}}'_{n\alpha}\,\hat{\boldsymbol{q}}_2) = 1/(4\pi)$.

Similarly to Eq. (B15 – B17), we define a function $\mathcal{G}^t_{n\alpha}$ which satisfies

$$\begin{aligned}\mathcal{G}^t_{n\alpha} =& \frac{1}{2}\int_{-1}^{1} dx\, \mathrm{P}_t(x)\, P^{-1}_{n\alpha} g_1(P_{n\alpha}) G^{(n)}_0(P_{n\alpha},q;E)\, g_0(P'_{\alpha n}) \\ =& \frac{1}{2}\int_{-1}^{1} dx\, \mathrm{P}_t(x)\, G^{(n)}_0(P_{n\alpha},q;E) \\ =& \frac{1}{2}\int_{-1}^{1} dx\, \mathrm{P}_t(x) \left[E - \frac{A+1}{2Am_n}\left(\frac{A^2}{(A+1)^2}q^2 + q'^2 + \frac{2A}{A+1}qq'x\right) - \frac{A+2}{2(A+1)m_n}q^2\right]^{-1} \\ =& \frac{m_n}{qq'}\,\mathrm{Q}_t(z_{n\alpha}) \end{aligned} \tag{B26}$$

with

$$z_{n\alpha} = \frac{1}{qq'}\left(m_n E - q^2 - \frac{A+1}{2A}q'^2\right) \ . \tag{B27}$$

After similar procedures to those used in calculating $\mathcal{Z}^{(0)}_{\alpha n}$, we can express $\mathcal{Z}^{(0)}_{n\alpha}$ as a summation of $\mathcal{G}^t_{n\alpha}$'s by

$$\mathcal{Z}^{(0)}_{n\alpha}(q,q';E) = \sqrt{3}\left(\frac{A}{A+1}q\,\mathcal{G}^0_{n\alpha}(q,q';E) + q'\,\mathcal{G}^1_{n\alpha}(q,q';E)\right) \ . \tag{B28}$$

c. *The Function $\mathcal{Z}^{(L)}_{nn}$ with $L = 0, 1$*

Also similarly, $\mathcal{Z}^{(L)}_{nn}$ is calculated as

$$\begin{aligned}\mathcal{Z}^{(L)}_{nn}(q,q';E) = &\iint p^2dp\,p'^2dp'\,g_1(p)G^{(n)}_0(p,q;E)\,g_1(p')\iint d^3p_1d^3q_1\iint d^3p_2d^3q_2 \\ &\times\ {}_n\langle p,q;\,(11)LM\,|\boldsymbol{p_1q_1}\rangle_n\,{}_n\langle\boldsymbol{p_1q_1}| - \mathcal{P}_{nn}|\boldsymbol{p_2q_2}\rangle_n\,{}_n\langle\boldsymbol{p_2q_2}|\,p',q';\,(11)LM\rangle_n \ .\end{aligned} \tag{B29}$$

The orbital-angular-momentum dependent matrix elements are written as

$${}_n\langle\boldsymbol{p_1q_1}|p,q;\,(11)LM\rangle_n = \frac{1}{p_1^2}\delta(p_1-p)\frac{1}{q_1^2}\delta(q_1-q)\mathcal{Y}^{LM}_{11}(\hat{\boldsymbol{p}}_1\hat{\boldsymbol{q}}_1) \ . \tag{B30}$$

The transition of momentum states in this case leads to

$${}_n\langle\boldsymbol{p_1q_1}| - \mathcal{P}_{nn}|\boldsymbol{p_2q_2}\rangle_n = -\delta^{(3)}(\boldsymbol{p}_1 - \boldsymbol{P}_{nn})\delta^{(3)}(\boldsymbol{p}_2 - \boldsymbol{P'}_{nn}) \ , \tag{B31}$$

where

$$\boldsymbol{P}_{nn} = \frac{\mu_{n\alpha}}{m_\alpha}\boldsymbol{q}_1 + \boldsymbol{q}_2 = \frac{1}{A+1}\boldsymbol{q}_1 + \boldsymbol{q}_2 \ , \tag{B32a}$$

$$\boldsymbol{P'}_{nn} = \boldsymbol{q}_1 + \frac{\mu_{n\alpha}}{m_\alpha}\boldsymbol{q}_2 = \boldsymbol{q}_1 + \frac{1}{A+1}\boldsymbol{q}_2 \ , \tag{B32b}$$

with $q_1 = q$ and $q_2 = q'$ determined from Eq. (B30).

We then rewrite Eq. (B29) as

$$\begin{aligned}\mathcal{Z}^{(L)}_{nn}(q,q';E) = -\int d\hat{\boldsymbol{q}}_1\int d\hat{\boldsymbol{q}}_2\,g_1(P_{nn})G^{(n)}_0(P_{nn},q;E)\,g_1(P'_{nn}) \\ \times\ \mathcal{Y}^{LM\,*}_{11}(\hat{\boldsymbol{P}}_{nn}\hat{\boldsymbol{q}}_1)\,\mathcal{Y}^{LM}_{11}(\hat{\boldsymbol{P}}'_{nn}\,\hat{\boldsymbol{q}}_2) \ .\end{aligned} \tag{B33}$$

As in Eq. (B15 – B17), we define the function $\mathcal{G}^t_{nn}$ that satisfies:

$$\begin{aligned}\mathcal{G}^t_{nn} =&\frac{1}{2}\int_{-1}^{1}dx\,\mathrm{P}_t(x)\,P^{-1}_{nn}\,g_1(P_{nn})G^{(n)}_0(P_{nn},q;E)\,g_1(P'_{\alpha n})P'^{-1}_{nn} \\ =&\frac{1}{2}\int_{-1}^{1}dx\,\mathrm{P}_t(x)\,G^{(n)}_0(P_{nn},q;E) \\ =&\frac{1}{2}\int_{-1}^{1}dx\,\mathrm{P}_t(x)\left[E - \frac{A+1}{2Am_n}\left(\frac{q^2}{(A+1)^2} + q'^2 + \frac{2qq'x}{A+1}\right) - \frac{A+2}{2(A+1)m_n}q^2\right]^{-1} \\ =&\frac{m_n}{qq'}\,\mathrm{Q}_t(z_{nn}) \ ,\end{aligned} \tag{B34}$$

with

$$z_{nn} = \frac{A}{qq'}\left[m_nE - \frac{A+1}{2A}(q^2+q'^2)\right] \ . \tag{B35}$$

Applying similar procedures again we express $\mathcal{Z}_{nn}^{(L)}$ as a summation of $\mathcal{G}_{nn}^{t}$'s. For $L=0$ and $L=1$, we obtain

$$\mathcal{Z}_{nn}^{(0)}(q,q';E) = -3\left[\frac{A^2+2A+4}{3(A+1)^2}qq'\,\mathcal{G}_{nn}^{0}(q,q';E) + \frac{1}{A+1}(q^2+q'^2)\,\mathcal{G}_{nn}^{1}(q,q';E) + \frac{2}{3}qq'\,\mathcal{G}_{nn}^{2}(q,q';E)\right] \tag{B36a}$$

$$\mathcal{Z}_{nn}^{(1)}(q,q';E) = qq'\,\mathcal{G}_{nn}^{0}(q,q';E) - qq'\,\mathcal{G}_{nn}^{2}(q,q';E)\ . \tag{B36b}$$

By substituting Eqs. (B20), (B28), and (B36) into Eq. (B4), we obtain the expressions for the kernel functions $X_{\alpha n}$, $X_{n\alpha}$ and X_{nn} given in Eqs. (58).

[1] I. Tanihata, J. Phys. G **22**, 157 (1996), and references therein.
[2] A. S. Jensen, K. Riisager, D. V. Fedorov and E. Garrido, Rev. Mod. Phys. **76**, 215 (2004), and references therein.
[3] M. V. Zhukov, B. V. Danilin, D. V. Fedorov, J. M. Bang, I. J. Thompson, and J. S. Vaagen, Phys. Rept. **231**, 151 (1993).
[4] I. Mazumdar, V. Arora and V. S. Bhasin, Phys. Rev. C **61**, 051303 (2000).
[5] G. Hagen, P. Hagen, H. -W. Hammer and L. Platter, Phys. Rev. Lett. **111**, 132501 (2013).
[6] S. C. Pieper, Nucl. Phys. A **751**, 516 (2005).
[7] S. Quaglioni, C. Romero-Redondo and P. Navrátil, Phys. Rev. C **88**, 034320 (2013).
[8] S. Bacca, N. Barnea and A. Schwenk, Phys. Rev. C **86**, 034321 (2012).
[9] M. Brodeur *et al.*, Phys. Rev. Lett. **108**, 052504 (2012).
[10] L. -B. Wang *et al.*, Phys. Rev. Lett. **93**, 142501 (2004).
[11] I. Tanihata, D. Hirata, T. Kobayashi, S. Shimoura, K. Sugimoto and H. Toki, Phys. Lett. B **289**, 261 (1992).
[12] G. D. Alkhazov *et al.*, Phys. Rev. Lett. **78**, 2313 (1997).
[13] O. A. Kiselev *et al.*, Eur. Phys. J. A **25**, 215 (2005).
[14] A. Ghovanlou, and D. R. Lehman, Phys. Rev. C **9**, 1730 (1974).
[15] D. R. Lehman, Phys. Rev. C **25**, 3146 (1982).
[16] S. Funada, H. Kameyama and Y. Sakuragi, Nucl. Phys. A **575**, 93 (1994).
[17] K. Varga, Y. Suzuki and Y. Ohbayasi, Phys. Rev. C **50**, 189 (1994).
[18] P. F. Bedaque, H. W. Hammer, and U. van Kolck, Nucl. Phys. A **676**, 357 (2000).
[19] P. F. Bedaque, H.-W. Hammer, and U. van Kolck, Phys. Rev. Lett. **82**, 463 (1999); Nucl. Phys. A **646**, 444 (1999).
[20] E. Braaten, and H. W. Hammer, Phys. Rept. **428**, 259 (2006).
[21] V. Efimov, Phys. Lett., **33B**, 563 (1970).
[22] N. Gross, Z. Shotan, S. Kokkelmans, and L. Khaykovich, Phys. Rev. Lett. **103**, 163202 (2009).
[23] S. E. Pollack, D. Dries, and R. G. Hulet, Science, **326**, 1683 (2009).
[24] T. Kraemer *et al.*, Nature **440**, 315 (2006).
[25] M. Zaccanti, B. Deissler, C. D'Errico, M. Fattori, M. Jona-Lasinio, S. Müller, G. Roati, M. Inguscio, and G. Modugno, Nature Physics **5**, 586 (2009).
[26] H.-W. Hammer, and L. Platter, Ann. Rev. Nucl. Part. Sci. **60**, 207 (2010).
[27] D. L. Canham, and H. -W. Hammer, Eur. Phys. J. A **37**, 367 (2008).
[28] D. L. Canham, and H. -W. Hammer, Nucl. Phys. A **836**, 275 (2010).
[29] M. T. Yamashita, T. Frederico, and L. Tomio, Phys. Lett. B **660**, 339 (2008).
[30] T. Frederico, A. Delfino, L. Tomio and M. T. Yamashita, Prog. Part. Nucl. Phys. **67**, 939 (2012).
[31] G. Rupak and R. Higa, Phys. Rev. Lett **106**, 222501 (2011)
[32] L. Fernando, R. Higa and G. Rupak, Eur. Phys. J. A **48**, 24 (2012).
[33] H. -W. Hammer and D. R. Phillips, Nucl. Phys. A **865**, 17 (2011).
[34] G. Rupak, L. Fernando and A. Vaghani, Phys. Rev. C **86**, 044608 (2012).
[35] B. Acharya and D. R. Phillips, Nucl. Phys. A **913**, 103 (2013).
[36] P. Hagen, H. -W. Hammer and L. Platter, Eur. Phys. J. A **49**, 118 (2013).
[37] X. Zhang, K. M. Nollett and D. R. Phillips, Phys. Rev. C **89**, 024613 (2014).
[38] C. A. Bertulani, H. W. Hammer, and U. Van Kolck, Nucl. Phys. A **712**, 37 (2002).
[39] P. F. Bedaque, H. W. Hammer, and U. van Kolck, Phys. Lett. B **569**, 159 (2003).
[40] V. Pascalutsa and D. R. Phillips, Phys. Rev. C **67**, 055202 (2003).
[41] R. A. Arndt, D. D. Long, and L. D. Roper, Nucl. Phys. A **209**, 429 (1973).
[42] G. Hale, *private communication.*
[43] J. Rotureau and U. van Kolck, Few Body Syst. **54**, 725 (2013).
[44] E. Braaten, P. Hagen, H. -W. Hammer and L. Platter, Phys. Rev. A **86**, 012711 (2012).
[45] Y. Nishida, Phys. Rev. A **86**, 012710 (2012).
[46] M. Jona-Lasinio, L. Pricoupenko, and Y. Castin, Phys. Rev. A **77**, 043611 (2008).
[47] M. C. Birse, J. A. McGovern, and K. G. Richardson, Phys. Lett. **B464**, 169 (1999).
[48] D. B. Kaplan, M. J. Savage, and M. B. Wise, Phys. Lett. **B424**, 390 (1998).
[49] U. van Kolck, Nucl. Phys. **A645**, 273 (1999).

[50] S. R. Beane, P. F. Bedaque, W. C. Haxton, D. R. Phillips, and M. J. Savage, "From hadrons to nuclei: Crossing the border," in the Borris Ioffe Festschrift, "At the frontier of particle physics: handbook of QCD", M. Shifman (ed.).
[51] P. F. Bedaque, and U. van Kolck, Ann. Rev. Nucl. Part. Sci., **52**, 339 (2002).
[52] D. E. Gonzalez Trotter *et al.*, Phys. Rev. C **73**, 034001 (2006).
[53] I. Šlaus, Y. Akaishi, H. Tanaka, Phys. Rept. **173**, 257 (1989).
[54] W. Glöckle, *The Quantum-Mechanical Few-Body Problem*, Springer-Verlag Berlin Heidelberg (1983).
[55] I. R. Afnan and A. W. Thomas, *Modern Three-Hadron Physics*, edited by A. W. Thomas, Springer-Verlag Berlin Heidelberg (1977), p1.
[56] L. D. Faddeev, Sov. Phys. JETP **12**, 1014 (1961) [Zh. Eksp. Teor. Fiz. **39**, 1459 (1960)].
[57] H. W. Hammer, and T. Mehen, Phys. Lett. B **516**, 353 (2001).
[58] C. Ji, D. R. Phillips, and L. Platter, Annals Phys. **327**, 1803 (2012).
[59] C. Ji and D. R. Phillips, Few Body Syst. **54**, 2317 (2013).
[60] J. Vanasse, Phys. Rev. C **88**, 044001 (2013).
[61] Arfken, G. "Neumann Series, Separable (Degenerate) Kernels", Chapter 16.3 in *Mathematical Methods for Physicists*, 3rd ed., Academic Press, Orlando, FL (1985).
[62] C. Ji, C. Elster, D. Phillips, *"Universal correlations in the ^{6}He ground state"* in progress (2014).
[63] K. Khaldi, C. .Elster, and W. Glöckle, Phys. Rev. C **82**, 054002 (2010).
[64] S. C. Pieper, R. B. Wiringa and J. Carlson, Phys. Rev. C **70**, 054325 (2004).
[65] C. Romero-Redondo, P. Navrátil, S. Quaglioni and G. Hupin, arXiv:1311.4595 [nucl-th].
[66] I. Tanihata *et al.*, Phys. Rev. Lett. **100**, 192502 (2008).
[67] A. R. Edmonds, *Angular Momentum in Quantum Mechanics* (Princeton U.P., Princeton, N.J., 1957).
[68] A more recent analysis of $n-\alpha$ data gives $a_1 = -65.7$ fm^3, $r_1 = -0.84$ fm^{-1} [42]. We have checked that using these values instead of those of Ref. [41] produces only very small differences in our results. Any such differences are certainly smaller than the intrinsic uncertainty in our leading-order calculation.